Matching ecohydrological processes and scales of banded vegetation patterns in semi-arid catchments

Athanasios Paschalis,[1,2] Gabriel G. Katul,[2,3] Simone Fatichi,[4] Gabriele Manoli,[2]

and Peter Molnar[4]

Athanasios Paschalis, Faculty of Engineering and the Environment, University of Southampton, UK (ap4c15@soton.ac.uk)

[1]Faculty of Engineering and the Environment, University of Southampton, UK

[2]Nicholas School of the Environment, Duke University, USA

[3]Department of Civil and Environmental Engineering, Duke University, USA

[4]Institute of Environmental Engineering, ETH Zurich, Switzerland

Abstract.

While the claim that water-carbon interactions result in spatially coherent vegetation patterning is rarely disputed in many arid and semi-arid regions, the significance of the detailed water pathways and other high frequency variability remain an open question. How the short temporal scale meteorological fluctuations form the long term spatial variability of available soil water in complex terrains due to the various hydrological, land surface and vegetation dynamic feedbacks, frames the scope of the work here. Knowledge of the detailed mechanistic feedbacks between soil, plants and the atmosphere will lead to advances in our understanding of plant water availability in arid and semi-arid ecosystems and will provide insights for future model development concerning vegetation pattern formation. In this study, quantitative estimates of water fluxes and vegetation productivity are provided for a semi-arid ecosystem with established vegetation bands on hillslopes using numerical simulations. A state-of-the-science process based ecohydrological model is used, which resolves hydrological and plant physiological processes at the relevant space and time scales, for relatively small periods (e.g. decades) of mature ecosystems (i.e. spatially static vegetation distribution). To unfold the mechanisms that shape the spatial distribution of soil moisture, plant productivity and the relevant surface/subsurface and atmospheric water fluxes, idealized hillslope numerical experiments are constructed, where the effects of soil-type, slope steepness and overland flow accumulation area are quantified. Those mechanisms are also simulated in the presence of complex topography features on landscapes. The main results are: (a)

Short temporal scale meteorological variability and accurate representation of the scales at which each ecohydrological process operates are crucial for the estimation of the spatial variability of soil water availability to the plant root zone; (b) Water fluxes such as evapotranspiration, infiltration, runoff-runon and subsurface soil water movement have a dynamic short temporal scale behavior that determines the long term spatial organization of plant soil water availability in ecosystems with established vegetation patterns; (c) Hypotheses concerning the hydrological responses that can lead to vegetation pattern formation have to accommodate realistic and physically based representations of the fast dynamics of key ecohydrological fluxes.

1. Introduction

In several arid and semi-arid regions around the world, vegetation communities assemble into organized spatial patterns primarily due to an interplay between key hydrological processes that facilitates plant growth at the patch scale but constrain the amount of biomass that can be sustained at spatial scales much larger than the patch size [e.g. *Klausmeier*, 1999; *Rietkerk et al.*, 2002; *Deblauwe et al.*, 2008; *Borgogno et al.*, 2009]. Common spatial structures include banded vegetation patterns [e.g. *Thiery et al.*, 1995; *Deblauwe et al.*, 2012] or other repeating patterns with isotropic spots or gaps (labyrinths) [e.g. *Couteron and Lejeune*, 2001; *Barbier et al.*, 2006; *Rietkerk and van de Koppel*, 2008]. Aerial photography and satellite imagery have shown that such vegetation patterning appears worldwide in many water-limited regions [e.g. *Deblauwe et al.*, 2008].

Several mechanisms have been hypothesized to explain the formation of such vegetation patterns [e.g. *HilleRisLambers et al.*, 2001; *van de Koppel et al.*, 2002; *D'Odorico et al.*, 2006a; *Saco et al.*, 2007; *Ursino*, 2007]. Many are primarily based on key hydrological processes that facilitate plant access to soil water though the precise pathway of water access may differ (e.g. lateral root access, infiltration contrast between vegetated and bare soil patches). Nevertheless, other candidate processes such as water and wind induced soil erosion and deposition have been proposed [e.g. *Valentin et al.*, 1999; *Okin and Gillette*, 2001; *Saco et al.*, 2007; *Saco and Moreno-de las Heras*, 2013]. A common feature among the proposed hypotheses is the existence of one or multiple mechanisms that provide a positive feedback to vegetation growth locally and a negative feedback as the spatial scale increases, thus leading to a pattern formation [*Borgogno et al.*, 2009; *Rietkerk and van de Koppel*, 2008].

Studies based on data analysis reveal interesting connections between climatology, geology, and vegetation pattern formations. Such work commonly seeks to obtain statistical descriptors between the spatial structure of vegetation patterns (e.g. shape, wavelengths periodicity, etc.) and meteorological (e.g. mean annual precipitation) or topographic and geological variables (e.g. terrain slope, distance from stream network, soil depth) [e.g. *Valentin et al.*, 1999; *Couteron*, 2002; *Ursino*, 2005; *Penny et al.*, 2013]. A major limitation to this analysis is data availability. Vegetation patterns commonly occur in sparsely gauged areas, where local meteorological records rarely exceed a few years, a time scale much shorter than the typical requirements for the organization of vegetation spatial structure. Patterns derived from aerial photographs or satellite imagery is also limited in terms of time span and thus the identification of the slow spatial dynamics of vegetation patterns is difficult.

Understanding the dynamic behavior of vegetation spatial patterns in response to climate change is gaining significance since precipitation regime, especially in terms of drought intensities and storm extremes, is expected to be largely affected in many semi-arid places of the world during the next century [*IPCC*, 2013; *Sillmann et al.*, 2013; *Kharin et al.*, 2013]. Hence, unfolding the hydrological processes that impact vegetation dynamics and their spatial organization in heterogeneous landscapes is becoming a necessity [*Rietkerk et al.*, 2004; *Kefi et al.*, 2007, 2008; *Thompson and Katul*, 2011].

The dynamical behavior of vegetation pattern formation has been explored using a number of simplified models [e.g. *HilleRisLambers et al.*, 2001; *Rietkerk and van de Koppel*, 2008; *Thompson and Katul*, 2009; *Mau et al.*, 2013]. All of these models are of reduced complexity, introducing simplifying assumptions for the vegetation dynamics and the hydrological processes (Figure 1) as well as uniformities in soil-plant properties. In particular, most of the

models conceptualize vegetation dynamics as a system of coupled partial differential equations (PDEs) of biomass density and water availability. Some further decompose water storage and flow into a fast surface component and a slower soil component. Even though the specifics of these PDEs differ, the way vegetation patterns emerge is due to short-range activation (a local facilitation) and long-range inhibition (a larger scale negative feedback) mechanisms [*Borgogno et al.*, 2009]. Another class of models for vegetation dynamics impose a set of rules forming a cellular automaton [e.g. *Dunkerley*, 1997; *Kefi et al.*, 2007; *Caracciolo et al.*, 2014; *van Wijk and Rodriguez-Iturbe*, 2002].

Some caveats common to the majority of those models are that (a) they consider a constant (or quasi-stationary) "meteorological" forcing on the system, an assumption far from being realistic, (b) operate on a time scale (e.g. years) irrelevant to the typical time scales of the hydrological processes (e.g. minutes-hours) or vegetation (e.g. days), that are crucial for water routing and ecosystem dynamics [e.g., *Pappas et al.*, 2015b], and (c) employ simplified representation of major hydrological and plant physiological processes. The present study targets those issues and explores their significance for semi-arid ecosystems that exhibit coherent vegetation patterns. Specifically, the questions being addressed here are: (1) Following variable rainfall events, what are the primary water pathways that interact with an established vegetation patten and likely preserve it? (2) how does meteorology, soil properties and topography affect those dynamics? and (3) are the results compatible with the behavior predicted by existing models of vegetation pattern formation?

Rather than explicitly simulating pattern emergence, the goal is to provide mechanistic explanations of vegetation functioning (i.e. water and carbon fluxes and stores) in semi-arid places where patterned systems already exist (i.e. vegetation is at equilibrium with the rainfall regime).

A mechanistic simulation of plant mortality, seed dispersal and establishment, which would lead to an explicit evolution of spatial vegetation dynamics while appealing is beyond the scope here. The above mentioned processes are, in fact, very uncertain and poorly simulated by existing ecosystem models [*Fatichi et al.*, 2015b]. In order to limit the numerical simulations to components which are better constrained, a fully mechanistic process based ecohydrological model, T&C [*Fatichi et al.*, 2012a; *Fatichi and Ivanov*, 2014] that solves most of the essential hydrological and plant physiological processes is used at their appropriate time scales. Numerical experiments for idealized hillslopes and real landscapes with established vegetation patterns are conducted in which water/energy fluxes and vegetation dynamics are modeled. The focus is primarily on banded vegetation systems, which are common in sloping terrains [e.g. *Lejeune et al.*, 2004; *Esteban and Fairén*, 2006; *McDonald et al.*, 2009; *Deblauwe et al.*, 2012]. However, as a result of the analysis, guidelines for simplified mechanistic ecohydrological modeling that can be used to predict dynamics of vegetation pattern formation are provided, and may represent the basis for future research.

2. Data and Methods

2.1. Data and Study Location

The study site is located in Western Texas (USA) near Fort Stockton (Figure 2). A well defined banded vegetation formation has been established [*Penny et al.*, 2013] consisting of drought resistant shrubs (e.g. tarbush), mixed mesquite, patches of sod grasses and Pinchot juniper [*McDonald et al.*, 2009]. Vegetation patterns occur primarily on the hillsides but are absent in steep locations and areas of high flow accumulation (e.g. streams). The established vegetation bands have a dominant periodicity of ~ 60 m (Figure 3c), with typical bare-soil and vegetation alternations of ~ 40 m and ~ 20 m respectively [*Penny et al.*, 2013]. Vegetation

structures have been identified using aerial imagery from the National Agriculture Imagery Program (NAIP) of the United States Department of Agriculture (USDA). A detailed statistical analysis of the vegetation patterns in this area can be found in *Penny et al.* [2013].

This semi-arid area experiences (i) about ~ 400 mm/year of precipitation unevenly distributed throughout the year (Figure 3a) and (ii) warm summers and mild winters. Precipitation is mostly concentrated in a few strong convective events occurring in summer and early fall, partially affected by the North American monsoon. The nearest records of hourly meteorological forcing (precipitation, temperature, relative humidity, incoming shortwave radiation and wind speed) were measured for the 1980-1990 period at the Midlands airport, located ~ 140 km North-East. Given the lack of strong orographic features between the selected study area and Midlands airport, the region in considered meteorologically homogeneous and the data are assumed to be representative for the study domain.

The geological formation within the study area can by classified into two distinct soil types: a low permeability silty-clay loam (soil type 1) and a high permeability silt loam (soil type 2) (Figure 2). In general, silty loam appears within the concave areas of the terrain and silt clay loam appears within the convex areas. The terrain is, on average, sloping with a minor inclination characterized by a hillslope gradient on the order of 0-4% (Figure 3b). Geological data were obtained by the USDA Soil Survey Geographic Database (SSURGO) and Elevation data by the National Elevation Dataset of the United States Geological Survey (USGS).

2.2. Model

The mechanistic ecohydrological model *T&C* is employed [*Fatichi et al.*, 2012a, b]. *T&C* is a state-of-the-science modeling tool that couples hydrological and plant physiological processes so as to resolve the water and energy balance, and the vegetation dynamics in complex terrains

and has been found to give very satisfactory results in various ecosystems worldwide, including semi-arid regions that are the focus of this study [*Fatichi*, 2010; *Fatichi et al.*, 2012a, b; *Fatichi and Ivanov*, 2014; *Fatichi et al.*, 2015a; *Paschalis et al.*, 2015; *Pappas et al.*, 2015a]. The major novelty of the present study in comparison to previous modeling approaches for ecosystems where vegetation patterns occur is the physically based representation of all the essential eco-hydrological processes, at least for ecosystems at a dynamic quasi-equilibrium (i.e. slow spatial vegetation dynamics in comparison to the time scales of the simulation and minor influence of the successional stage of the ecosystem). For this reason the uncertainties related to empirical assumptions (generally employed in existing models of vegetation pattern formation) and their impact on the natural system feedbacks should be considerably reduced in the present study. Moreover, a realistic process representation can quantify in detail the composite effect of meteorological variability (e.g. precipitation, temperature, atmospheric humidity, radiation and wind speed) at the correct temporal scales [*Paschalis et al.*, 2015]. Even though previous studies dealing with forcing variability in vegetation patterns exist [e.g. *Kletter et al.*, 2009; *Baudena et al.*, 2013] the present study introduces an integrated framework that is expected to provide a more thorough insight on ecosystem functioning.

The hydrological processes resolved in *T&C* are: radiation patterns in complex terrain and radiation transfer though the canopy, interception, throughfall, infiltration, a quasi 3 dimensional soil water redistribution solving a vertical Richards equation [*Abarbanel et al.*, 1993; *Hopp et al.*, 2015] (1D - quasi 3D formulation with plant water uptake sinks vertically distributed according to an exponential decay function). Preferential flows are not simulated, while rainfall can induce soil sealing formation. Overland water routing is solved with the kinematic wave form of the Saint-Venant equations. Additional simulated processes are snow hydrology, and a

complete solution of the energy balance in the vertical direction for the quantification of heat fluxes between the land surface and the atmospheric boundary layer. Spatial discretization of the watershed is achieved on a squared lattice, and temporal discretization depends on the specific hydrological process.

The vegetation component of the model calculates in a prognostic manner the plant biomass in 7 different carbon pools (e.g. leaves, fine roots, living sapwood, carbohydrate reserves, dead leaves, heartwood and fruits/flowers). Changes in carbon pools are the result of the balance between carbon gains (photosynthesis), and losses (respiration and tissue turnover) and their temporal dynamic behavior is thus fully captured. Biomass is allocated and translocated between various carbon pools following a set of rules that take into account resource distribution, plant allometric constraints, and plant phenology. The model conceptualizes vegetation using either broad category plant functional types ($PFTs$) [e.g. *Haxeltine and Prentice*, 1996; *Bonan et al.*, 2002; *Sitch et al.*, 2003; *Krinner et al.*, 2005] or defined specific plant parameters [*Fatichi and Leuzinger*, 2013; *Pappas*, 2014; *Pappas et al.*, 2015a], taking into account structural and physiological differences between species. Vegetation can be structured into 2 layers (overstory and understory) and multiple vegetation types can cover each computational cell. In the current version of the model, forest demography, spatial vegetation dynamics and soil biogeochemistry are not taken into account. The model thus assumes mature ecosystems in equilibrium with the local mineral nutritional status. Even though the model does not simulate spatial dynamics of vegetation (e.g. establishment over new vegetated areas) those occur on long temporal scales ($\sim$ decades) and do not represent the scope of the present study. The focus is on the short term responses of established vegetation patterns to the spatial variability of water fluxes, which is the first necessary step for all subsequent computations of spatial distributed dynamics. In other

words, in order to simulate in a realistic manner slow processes such as spatial vegetation dynamics, the soil water availability to plants in a quasi-equilibrium vegetation state should be correctly captured. Also, plant hydraulics are not explicitly taken into account, and phenomena such as xylem cavitation/embolism or hydraulic lift are not simulated.

Due to the complexity of the process representation in *T&C*, the computational demand can be prohibitive, limiting the capability of long term simulations and sensitivity analysis. Moreover, given the limited knowledge of the boundary conditions within the study area, two main simplifications to the original formulation of the model are introduced. The computationally demanding solution of the energy balance, which leads to the estimation of the sensible, latent and ground heat fluxes was changed to an analytical solution similar to the one used in *Shuttleworth and Wallace* [1985]. For the estimation of evapotranspiration, this model has been successfully used in hydrological and ecological studies [e.g. *Brisson et al.*, 1998; *Iritz et al.*, 1999; *Zhou et al.*, 2006]. The main limitation of this simplification is the simulation of only one vegetation layer per computational cell, contrary to two in the original model formulation. For the examined semi-arid area here, this may not be an issue except in locations where tall vegetation (e.g. bushes or trees) co-exist with understory grasses. Another limitation inherent in the Shuttleworth and Wallace model is the single big leaf approximation, which is different from the two big leaves (sun-shaded) approximation in the current formulation of *T&C*.

The second, more relevant, simplification introduced is a lumped, depth averaged representation of soil hydrology within the root-zone. This results in a single bucket-type model, a common assumption in hydrological and early dynamic global vegetation models [e.g. *Laio et al.*, 2001; *Sitch et al.*, 2003; *Daly and Porporato*, 2006; *Gerten et al.*, 2004; *Ghannam et al.*, 2016]. Specifically, the soil moisture in the root-zone is modeled using the mass balance:

$$Z_r \frac{d\overline{\theta}}{dt} = I - ET - L + S_l,$$

where Z_r $[L]$ is the root zone depth assumed constant, $\overline{\theta}$ $[L^3L^{-3}]$ is the root-zone averaged volumetric water content, I $[LT^{-1}]$ is the water infiltration into the soil, ET $[LT^{-1}]$ is the evapotranspiration, L $[LT^{-1}]$ is the leakage to deeper soil layers or bedrock assumed to vary with θ, and S_l $[LT^{-1}]$ is the net lateral soil water exchange. This simplification reduced the computational time substantially and removed uncertainties associated with the vertical structure of the root system. The I is modeled as a function of the water content similar to the original modeling procedure of *T&C* [*Fatichi et al.*, 2012a]. The ET is modeled according to the resistance scheme presented in *Shuttleworth and Wallace* [1985], where an analytical solution for the evaporation fluxes for sparse canopies is presented. Aerodynamic [*Choudhury and Monteith*, 1988], leaf boundary layer [*Shuttleworth and Gurney*, 1990] and stomatal resistances [*Leuning*, 1995] are estimated using formulations identical to the original *T&C*, whereas soil resistance is related to the average water content within the root zone. The L is related to the soil hydraulic conductivity and the soil water content, and finally S_l is described by the sum of the lateral soil fluxes at every computational cell from and to its neighbors according to a depth averaged representation of Richards equation. This assumption simplifies soil water movement - and allows a detailed representation of lateral water exchanges along the main dimension experiencing soil water variability - the hill slope. The consequences of employing those two simplifications are further examined and discussed in the context of the idealized hillslope. A detailed description of the simplifications are provided in appendix A.

In total, 5 different time steps are employed in the numerical scheme. Vegetation dynamics are solved at the daily time scale, energy fluxes at the hourly time scale, soil crust formation

at a 5 minute time scale, soil water content, infiltration and runoff production are estimated with an adaptive time step based on a maximum allowed water content difference ($\sim$ seconds - 5 min), and overland flow routing is computed with an adaptive time step that satisfies the Courant-Friedrichs-Lewy condition [*Hunter et al.*, 2005] ($\sim$ seconds - 5 min). Precipitation disaggregation from a 1 hour to a 5-minute interval is performed with a stochastic multiplicative random cascade model [*Paschalis et al.*, 2014; *Paschalis*, 2013].

2.3. Numerical simulations

The goal is to provide a quantification of the hydrological response to climatic variations of a watershed where coherent vegetation patterns have been established. The key variables considered are steepness of the slopes and the soil hydraulic properties. To isolate the influence of those variables, a set of numerical simulations for an idealized one-dimensional hillslope are first constructed, followed by simulations that account for realistic topography so as to assess the influence of the complex terrain.

2.3.1. Idealized slope setup

The first set of numerical experiments refer to a simplified hillslope (semi-infinite plane) with a unique slope ϕ (Figure 4). Along the slope, vegetation bands are imposed with a periodicity of 62 m (Figure 3c) and with a band width of 16 m. This configuration roughly resembles the mean band properties estimated from aerial imagery by *Penny et al.* [2013] for the case study site. Slopes are allowed to vary in the range 0.5%-5% (Figure 3b), a typical range where banded vegetation patterns commonly occur [e.g. *Couteron et al.*, 2000; *Lejeune et al.*, 2004; *Thompson et al.*, 2008a]. Vegetation properties are selected to represent the most abundant species in the study area, and are parametrized as a PFT representing an evergreen shrubland. The same *T&C* parametrization for this plant type has been found to provide acceptable results in semi-

arid areas with a climate similar to the study location here [*Fatichi et al.*, 2012b; *Fatichi and Ivanov*, 2014]. The inherent assumption behind the simulations in this study is that vegetation patterns are in equilibrium and not in a transient phase adapting to a new precipitation regime, or recovering from some recent large scale disturbance (e.g. fire). This is essential since spatial movement of vegetation are not modeled by *T&C*, but their local dynamics are. This assumption is not easy to validate. However, indirect support is provided by aerial photographs spanning 20 year (available through Google Earth record - not reported here) over the study region that suggest no appreciable change in vegetation structure. This evidence is consistent with the assumption that vegetation is at equilibrium in this area.

The length of the slope is 1 km thereby allowing investigation of the effect of water accumulation due to overland flow. The spatial discretization is 2×2 m^2. Due to the homogeneity of the shape of the idealized slope no water fluxes occur in the y direction (Figure 4) and for this reason only a narrow slope of 2 m was taken into account. Due to the relatively small size of the computational grid, spatial homogeneity was assumed within every cell, eliminating the need to define a fractional plant cover. Moreover, the root system of every vegetated cell is assumed to extend only vertically and not to expand laterally to neighboring cells. Given the small size of the shrubs covering the study area and the lack of detailed belowground information, this assumption may be reasonable.

Soil hydraulic properties are estimated using the pedotransfer functions of *Saxton and Rawls* [2006], which describe the saturated hydraulic conductivity and the shape of the soil water retention curve as a function of soil textural properties and soil organic matter content. In semi-arid environments, vegetated areas are known to have higher hydraulic conductivity, which typically leads to enhanced infiltration rates and higher water holding capacity [e.g. *Ludwig*

et al., 2005; *Madsen et al.*, 2008; *Franz et al.*, 2012; *Foti and Ramírez*, 2013]. This behavior is modeled by prescribing a higher organic matter percentage in the soil below vegetated cells (Table 1). Two different soil types accounting for the two major categories featured at the study site are considered. Anisotropy is accounted for assuming the hydraulic conductivity in the vertical and horizontal directions with a ratio $K_v/K_h = 0.1$ for the first soil type and $K_v/K_h = 0.2$ for the second. Even though the anisotropy of hydraulic conductivity is known to depend on soil saturation [*Assouline and Or*, 2006], it was assumed to be a constant due to the absence of additional information. The root zone depth is set to 0.6 m. For the first soil type, leakage to deeper soils is allowed, whereas for the second, leakage is suppressed due the shallow soil depth reported in *Penny et al.* [2013]. A dynamic formation of a rainfall induced soil seal is also modeled according to the model presented by *Assouline and Mualem* [1997, 2000]; *Assouline* [2004], and applied by *Fatichi et al.* [2012a]. Even though different processes may lead to the formation of a soil crust (e.g. biological or chemical crust) [e.g. *Agassi et al.*, 1981; *Belnap*, 2006], only rainfall induced soil sealing is modeled considering that the other mechanisms may have similar effects on infiltration suppression.

In the Supporting information, the effect of precipitation is analyzed using three different scenarios where the total precipitation amount is considered equal, half and double of the observed. The purpose of those precipitation scenarios is not to reflect bounds on realistic climate scenarios for the study area since the equilibrium hypothesis is invalidated by such large precipitation changes. These scenarios are only intended for assessing the sensitivity of the ecohydrological feedbacks between the prescribed biomass distribution in space and the (fast) hydrological processes impacting them.

For each case, a spin-up simulation of one year was used to obtain realistic initial soil moisture conditions in statistical equilibrium with the prescribed precipitation. A summary of the numerical set-up is provided in Table 1.

2.3.2. Landscape analysis setup

The numerical experiments for the reduced topographic complexity case provide basic background about the hydrological response of a hillslope with an established vegetation pattern. However, to what degree those result can be observed (or not) in reality is an open question since the complexity of the terrain introduces additional degrees of freedom. The two main signatures of topography are radiation distribution and lateral surface and subsurface water flow. To investigate those influences, two different areas with a 1 km^2 size, located within the study domain are selected (Figure 5). The two areas have different soil hydraulic properties. For the simulation of those two areas, only observed meteorological forcing is considered. Also, due to the difficulty in defining water fluxes at boundaries of the simulation, a zero water flux boundary is assumed for both cases to ensure conservation of water mass. In these simulations, vegetation is also considered in equilibrium with the prescribed precipitation and climate forcing for the entire period of the simulation (i.e. no evident changes in vegetation location and structure occur during the simulation period).

3. Results and Discussion

3.1. Effects of Model Simplifications

Potential biases due to simplifications applied to the original model are examined against the full version of *T&C* for the idealized slope (section 2.3.1) with an inclination of 1% and a 200 m length. Vegetation bands identical to the ones described in section 2.3.1 are prescribed. The soil is set to the more permeable soil type (i.e. soil type 2), which is expected to introduce the largest

possible bias following the aforementioned simplifications. In all cases, the meteorological time series is taken from the observed data (section 2.1). The model comparison focuses on two components where the simplifications are introduced - the estimation of evapotranspiration and the dynamics of water movement within the soil.

Modeled latent heat fluxes (ET) and soil moisture dynamics between the two versions of the model are in good agreement (Figure 6). In particular, ET differences between the two models are unbiased with small spread (Figure 6a) around the one-to-one line ($R^2 = 0.86$, evaluated at the daily scale), showing that the ET approximation using the Shuttleworth and Wallace model is satisfactory for this ecosystem. The comparison between the soil moisture dynamics is also acceptable (Figure 6b). Soil moisture dynamics modeled with the simplified version for bare soil patches are almost identical to the full model, which solves the quasi-3 dimensional soil water movement in the soil in multiple soil layer depths (vertical discretization: depth 0-50 mm with 10 mm steps and depths from 50-600 mm with 50 mm steps). Small discrepancies concerning the soil moisture dynamics for the vegetated patch do exist but their effects are small when compared to the overall variability of soil moisture across grid cells along the hill slope. Also, given that the plant physiological components are identical between the two model versions, those discrepancies can be attributed (a) to the assumption of one versus two big leaves between the two models, and (b) to the vertical distribution of the soil moisture and its connection to the vertically distributed water variable root uptake function, which is neglected in the simplified model. The latter affects plant transpiration and drought stress in a non-linear way due to the exponential root density profile assumed in the full model. Not withstanding these differences, the comparison is satisfactory and suggests that the simplified model can serve as an adequate tool for the purposes of the present study without any major information losses

in terms of soil moisture dynamics. It should be noted that intermediate complexity models for soil water dynamics that adopt 2 soil layers (surface and deep) have been also presented to investigate semi-arid ecosystems [e.g. *Baudena et al.*, 2013; *Vico et al.*, 2014]. However, given the acceptable agreement between the single bucket model and the complete 3-dimensional solution to Richards equation with non-uniform root-density profiles (Figure 6b), we believe that even a single bucket can be considered sufficient for the purpose of this study.

3.2. Idealized Slope Analysis

3.2.1. Ecohydrological response: Time-averaged patterns

Profiles of the time-averaged water fluxes and state variables (e.g. soil moisture) are presented in Figure 7 for the two main soil types. In all cases, the soil moisture below vegetated patches is, on average, less than the their adjacent bare soil neighbors (Figure 7a). This contradicts previous hypotheses that vegetated patterns can maintain higher soil water amounts [e.g. *D'Odorico et al.*, 2006b] (Figure 1), a common result in several vegetation pattern formation models. The result we report here is in agreement with the type of models similar to [*Klausmeier*, 1999] as presented in *Ursino* [2007] or the competition scenario of the model presented in *Gilad et al.* [2007a] but in disagreement with several other models [e.g. *HilleRisLambers et al.*, 2001; *Gilad et al.*, 2007b]. This result also contradicts a few field studies [e.g. *Bhark and Small*, 2003; *Greene*, 1992; *D'Odorico et al.*, 2007] that suggest soil moisture may be higher in vegetated patches in semi-arid regions where vegetation patterns occur. The work by *Ursino* [2007] underlined that the spatial distribution of soil moisture is dependent on the parameterization of the component linking soil water availability and vegetation growth. Given that vegetation growth is based on a detailed representation of physical and biochemical processes here, the results

in this study can provide some perspective on these contradictory results as they pertain to the temporal dynamics of water movement.

The reason why low soil moisture occurs in vegetated patches is that ET losses within vegetated areas are higher than their bare soil neighbors (Figure 7c). Water gained from either enhanced infiltration (Figure 7b) or subsurface water routing (Figure 7f) appears to be insufficient for providing excess water beyond the enhanced ET demand. ET is, on average, high due to the combined effect of bare soil evaporation, and plant transpiration. In bare soil, atmospheric water vapor demand is solely met due to bare soil evaporation, which can be highly inefficient at low soil moisture [e.g. *Haghighi et al.*, 2013; *Or et al.*, 2013]. This effect would have been more pronounced if the full profile of the soil water content was taken into account, given that the efficiency of the bare soil evaporation depends on water content status near the soil surface, which in semi-arid environments, is lower on average than the root-zone soil moisture. On the contrary, in vegetated patches, atmospheric water vapor demand is met both by soil water evaporation and plant transpiration. Transpiration is an effective process, especially for drought resistant plants that close their stomata at negative soil water potential lower than -2 MPa [e.g. *Sperry*, 2000; *Guyot et al.*, 2012]. Transpiration is also less sensitive than bare soil evaporation to the low soil water availability near the surface as plants can access deeper soil layers. Moreover, in semi-arid places where vegetation patterns occur, bare soil evaporation is not severely limited in vegetated areas, due to the prevelance of high available energy at the ground and low values of leaf area index leading to low light interception within the canopy. Evaporation from interception, another component of total ET, was found to be small ($\sim$ 10 mm/year considering the precipitation amount) due to the low leaf area index and rare precipitation events.

The directionality of water fluxes leading to the aforementioned soil moisture variation is of major significance. It was shown that the dominant flux that leads to decreased soil water availability in vegetated patches is ET, which is approximately equal to the total incoming water ($ET \approx I + S_l$) as the study area lies on the water limited regime of Budyko's curve [*Wagener et al.*, 2007; *Fatichi and Ivanov*, 2014]. Therefore, it is thus crucial to quantify the magnitude and direction of runoff and subsurface water fluxes that affect I and S_l respectively. In Figure 7(b-f), the time averaged behavior of those fluxes is shown.

Long-term infiltration larger or lower than precipitation can only occur when there is runoff production and due to overland flow water is transfered from upstream and is made available to downstream areas. The pattern of infiltration is similar for both soil types investigated here (Figure 7b). In the upstream portions of a vegetated patch, infiltration is higher on average. The mechanism that leads to this behavior is as follows: (1) runoff, mostly as infiltration excess (Horton runoff), is generated in the bare soil areas and routed downstream. Runoff production is higher in bare soil areas due to their lower permeability and more frequent soil sealing formation in comparison to the neighboring vegetated areas (Figure 7e). (2) Vegetated areas with a higher infiltration capacity can gain water produced by the upstream bare soil areas. (3) Given the comparable time scales of water routing and the infiltration process, uphill areas of each vegetation band have the potential of gaining more water from upstream runoff. This effect can only occur when runoff is ephemeral, of small magnitude and the slopes are shallow, which leads to overland flow velocities comparable with infiltration rates. If runoff becomes continuous, or surface velocities become large (e.g. steep terrain), the observed anisotropy could ameliorate. The present result concerning runoff and enhanced infiltration in vegetated areas

of a banded ecosystem supports results from simplified models predicting vegetation pattern formation (Figure 1).

The second source (or sink) of soil moisture is subsurface soil water movement. The time averaged behavior for net gain/losses of soil water through subsurface movement shows a more complex pattern (Figure 7f), which is related to precipitation and to a lesser extent, slope steepness. On average, edges of vegetated areas are sinks of soil water. This can be attributed to their lower soil water content, which then results in a gradient of soil water potential and enhanced suction that can operate against the (small) topographic gradient. The influence of lateral soil water fluxes can be comparable in magnitude to the effects of runoff, especially in soils with high permeability (Figure 7e-7f). This is primarily true at the interfaces between vegetated and bare soils, where the pressure gradients are maximum. The fact that vegetation edges act as soil water sinks has an apparent effect on ET and carbon assimilation (GPP) (Figure 7(c,g)), resulting in an anisotropic behavior that partially counteracts the effect of runoff, since in this case the downstream sink is stronger. Enhancement of GPP at the edges also result in increased modeled biomass (not shown here). This balance between the effects of the two fluxes and the involved magnitudes can potentially be significant for vegetation band migration and/or establishment and mortality.

There is evidence that banded vegetation migrates uphill [e.g. *Deblauwe et al.*, 2012; *Thompson et al.*, 2008b]. Given that in semi-arid places the strongest limitation for plant survival is soil water availability, the results presented here lay a template for the spatial dynamics of vegetation. Vegetation is expected to migrate to places were resource availability is higher. Our results (Figure 7) indicate a small relative advantage in areas uphill of vegetation bands, since soil moisture is on average higher in the uphill locations than downhill, and those areas received

generally more water from runon. Concurrently, the commonly observed upslope migration could be attributed to less favorable soil water availability at the lower part of each band, which could lead to enhanced plant stress and eventually mortality. This hypothesis has to be confirmed in future research by adopting models that include physically realistic representations of plant mortality, a major open question in ecohydrology. However, another important aspect is that the average soil patterns hide key features of the dynamical behavior of the water fluxes and thus soil water availability, which are discussed next.

3.2.2. Temporal dynamics of the water fluxes

To explain the patterns presented in Figure 7, the analysis of the temporal evolution of the soil moisture is now considered. This will highlight the influence of the temporal variability of the meteorological forcing, a factor commonly neglected in the investigation of the dynamics of vegetation pattern formation with few exceptions [e.g. *D'Odorico et al.*, 2006a; *Konings et al.*, 2011; *Baudena et al.*, 2013; *Kletter et al.*, 2009].

In Figure 8, the dynamic behavior of soil water content for the upper, lower, and middle part of a vegetation band as well as their adjacent bare soil are shown. Simulations correspond to the case of a silty-clay loam with a slope inclination of 1%. The selected points are located approximately in the middle of the hillslope. By exploring variability of soil moisture, the dynamic behavior of the relative contributions of ET, runoff, and subsurface flow across a gradient of declining drought stress can also be explored.

The dynamics of the water fluxes are complicated when overland flow is generated by the hillslopes (Figure 8c-d). In semi-arid places, runoff is primarily Hortonian and occurs only after intense storms. Following the occurrence of these intense storms, infiltration capacity of the bare soils is reduced due to soil sealing. When overland flow occurs, the ecosystem takes

advantage of enhanced infiltration capacity of the soil in the vegetated areas. These mechanisms contribute to enhanced root-zone soil moisture. The duration of the more favorable soil moisture conditions in the vegetated areas relates to the amount and occurrence of runoff (Figure 8c-d). Due to the fact that in semiarid hillslopes the overland flow magnitude is small, and flow velocities are relatively slow, the uphill parts of the vegetation bands have some advantage in harvesting more water than their immediate downhill counterparts, leading to the anisotropy shown in Figure 7b,e. However, this advantage does not lead to substantially different soil moisture conditions for the uphill areas because it dissipates relatively fast ($\sim$ few days).

When runoff occurs, the subsurface lateral flow has a heterogeneous spatial and temporal behavior, when compared to cases where no runoff occurs and lateral subsurface water fluxes have a constant direction in time (Figure 8b). The flow direction here has three basic phases (Figure 8e). During long dry periods, where soil moisture is lower in the vegetated patches and thus the water potential is lower than its neighboring bare soil areas, water is moving towards the vegetated areas. During a storm that generates runoff, vegetated patches receive more water due to enhanced infiltration that gradually shifts them from water sinks to sources. After a significant storm, soil moisture is higher in vegetated areas and during the post-storm period, this area is supplying water to the drier soil neighbors until the larger ET dries the vegetated patches again. Also the flow direction within the patch is modified during and after an intense rainfall event due to the advantage in water gain from uphill locations. The complex average profiles of water gain/loss shown in Figure 7f integrate this dynamic behavior induced by short temporal scale (minutes to hours) variability of precipitation. This integrated behavior depends on the ability of precipitation to generate runoff and the duration the system resides in those three states, which in turn depends on soil hydraulic properties and to a smaller degree topography (i.e. slope

steepness). This time dependent behavior of the lateral water fluxes highlights the importance of the temporal organization of storms and their intensities [e.g. *Noy-Meir*, 1973; *Baudena et al.*, 2013; *Paschalis et al.*, 2015] and to some degree can explain the discrepancies with some field based studies [e.g. *D'Odorico et al.*, 2007; *Bhark and Small*, 2003]. In particular, more frequent precipitation, but not necessarily enhanced precipitation in terms of annual accumulation, could potentially lead to higher soil moisture in vegetated patches for longer times, since the heterogeneous infiltration mechanism would be activated more often. Moreover, the complicated temporal dynamic behavior of the water fluxes indicates that field based studies should be performed in a time continuous manner, and a direct comparison with field experiments of limited temporal duration is possibly problematic (and biased).

In all cases, soil leakage to deeper layers was small, occurring only after major precipitation events and was found not to be crucial for shaping the spatial patterns of soil moisture, and thus is not further discussed.

3.3. Landscape analysis

The previous simulations for the idealized hillslope with unique inclination allowed to quantify the dynamics of water fluxes and the ecohydrological responses of ecosystems with established banded vegetation structure. A major question is whether such a behavior can be observed when the influence of a real complex topography is taken into account. For this reason simulations of two locations with a 1 km^2 size within the selected study domain were carried out (Figure 5). Larger computational requirements limit us to a selection of 4 years for catchment distributed simulations.

It can be shown that magnitudes in terms of water and carbon fluxes are comparable to the idealized hillslope and manifest themselves on the complex topographic features (Figure 9).

For both simulated areas, vegetated patches maintain, on average, a lower soil water content than their bare soil neighbors (Figure 9a). The differences between the soil moisture between vegetated and bare soils gradually declines with flow accumulation area.

Enhanced infiltration in areas where vegetation is present appears with both soil parametrizations adopted in the study. The infiltration contrast is generally stronger in areas where overland flow contributing area is small and vanishes in areas with higher contributing areas. Therefore, the water competing mechanisms that lead to vegetation pattern formation become weaker where overland flow concentrates. This finding may be suggestive as to why vegetation patterns occur on flat areas or hillslopes and not close to streams (e.g. Figure 2).

Patterns of subsurface gain or loss of water (Figure 9c) also exhibit the same spatial structure as in the case of the idealized hillslopes. Edges of vegetation bands act as net sinks of soil water and nearby bare soil areas act as water sources. In this case, the topography seems to play a minor role and the flow accumulation effect are not apparent as in the case of infiltration. A plausible explanation is that for the shallow terrain presented here, the sharp differences of water matric potential between vegetated and bare soil areas dominate the flow direction in comparison to gravitational water potential gradients induced by elevation differences.

Finally, the combined effect of enhanced infiltration and subsurface water flow result in a spatial pattern of carbon assimilation (Figure 9d). This pattern shares similar features with the idealized hillslope case characterized by a single inclination. Increased carbon gain occurs in areas of overland flow accumulation due to enhanced infiltration and on edges of each patch due to subsurface water contribution to vegetated areas. Note that differences in local GPP can be on the order of 30-50% (Figure 9)

4. Outlook

4.1. Towards a mechanistic model for vegetation pattern formation

The findings here highlight the usefulness of models that explicitly account for the main eco-hydrological responses of ecosystems and solve temporal and spatial dynamics of water fluxes at appropriate spatial and temporal scales. Up to now, the majority of approaches investigating the spatial dynamics of vegetation pattern formation has been confined to reduced complexity, conceptual models with a small degree of physical realism. A few attempts aimed at improving the process representation in such modeling framework [e.g. *Foti and Ramírez*, 2013; *Gutiérrez-Jurado et al.*, 2013; *Caracciolo et al.*, 2014; *Flores Cervantes et al.*, 2014]. It is not our intention to understate the value of these idealized models. In fact, these aforementioned models motivated the detailed process based approach with dynamic components for vegetation (but not spatial) explored here.

However, our results clearly indicate that various features of the water and carbon cycles and the feedbacks between the two ultimately shape the spatial patterns of water availability to the plants in semiarid regions. In order to capture such features, hydrological and plant physiological processes have to be resolved at their appropriate temporal scales which may span from second up to decades. Most important, our results indicate that the short temporal scale responses to meteorological variability very likely shape the long term spatial patterns of water availability in ecosystems that have established vegetation patterns. For this reason short temporal scale features of meteorological forcing (e.g. rainfall pulse durations, heat waves etc) cannot get lumped in a single diagnostic variable (e.g. mean annual rainfall), if mechanisms of vegetation pattern formation have to be understood and modeled. In order to advance models for such ecosystems and aim at mechanistic descriptions that lead to vegetation pattern generation we need ti

integrate knowledge from catchment hydrology [e.g. *Rigon et al.*, 2006; *Shen and Phanikumar*, 2010; *Fatichi et al.*, 2012a], modeling of carbon pools, pioneered by global vegetation studies, [e.g. *Friend et al.*, 1997; *Sitch et al.*, 2008], plant demography [e.g. *Moorcroft et al.*, 2001; *Bugmann*, 2001], plant seed dispersal [*Nathan and Muller-Landau*, 2000; *Katul et al.*, 2005; *Thompson et al.*, 2014], and geomorphology [e.g. *Francipane et al.*, 2012; *Yetemen et al.*, 2015] at appropriate temporal and spatial scales. Unfortunately, a complete understanding of these processes, the data availability, and the computational demand still represent insurmountable obstacles and leave such modeling framework as a task for the future.

It may be conjectured that the main processes that must be resolved in this future endeavor include: (1) Plant seed production and dispersal. To estimate plant seed production, a mechanistic vegetation model should also simulate seed dispersal mechanisms, which are species dependent and include various contributions such as dispersal by wind, secondary transport mechanisms from runoff [e.g. *Thompson et al.*, 2014] or animals. (2) Germination and establishment. The probability of seed germination and sapling establishment, which is dependent on resource availability (water, light, nutrients) and resource competition must be included. (3) Plant mortality. Modeling of plant mortality is an essential but very difficult component to model, especially when drought induced mortality is a key element [e.g. *McDowell et al.*, 2011, 2013]. (4) Soil erosion and soil biogeochemistry. The absence of vegetation in the soil affects its erosion rate as well as its chemical and biological functioning. This can have implications for crust formation, and also affect the nutrient status of the soil, an essential feature for vegetation functioning. The dynamic balance between establishment and mortality is the dominant mechanism that leads to a spatial dynamic behavior of vegetation and thus pattern formation. Note the all of the above processes are in turn affected by soil moisture and there-

fore linked to the results of our analysis. All these processes also operate on different time scales. For example, seed abscission and secondary seed dispersal by runoff, are controlled by small scale meteorological variability. To the contrary, the consequences of changes in soil biochemistry and geomorphic processes (e.g. soil erosion) operate on longer times scales. For this reason, an appropriate coupling that takes into account this scale separation is essential as it is the stochastic nature of some of the processes involved (e.g. seed germination) which would therefore require averaging a consistent number of simulations to obtain meaningful results.

4.2. Limits of Interpretation

The study was based on numerical simulations only and several assumptions were made. The two major implications arise from (1) the representation of hydrological and plant physiological processes in the model, and (2) the assumptions concerning the system boundary conditions and model parameters (e.g. soil hydraulic properties, model parameters related to vegetation processes etc.).

Most hydrological processes (e.g soil water and surface flow, interception, throughfall, ET), have commonly accepted physically-based modeling procedures. The most critical representations that potentially influence the results reported in the present study concern the mechanisms leading to soil surface sealing during rainfall events, and the lumped representation of the water balance in the root zone. Specifically, even though in semi-arid places, soil surface crust is often present due to various biological, chemical and physical factors, only one mechanistic model has been presented with a series of simplifying assumptions and uncertain parameters [*Assouline and Or*, 2006; *Fatichi et al.*, 2012b]. Accounting for alternative types of soil crusts may reduce the impact of the infiltration contrast between vegetated and bare soils, which could potentially modify the presented results. A combination of field based quantification of the ex-

istence and strength of the different types of soil crust and its comparison with current models can provide important insight for vegetation pattern formation. Also, the lumped representation of soil hydrology can influence the results since the vertical profile of soil moisture is not simulated, and the detailed effect of the highly nonlinear dynamics describing soil water flow is not explicitly represented [e.g. *Guswa et al.*, 2002; *Kurc and Small*, 2004; *Cavanaugh et al.*, 2011].

In contrast to hydrological processes, mechanistic modeling of vegetation processes has less commonly accepted parameterizations and still represents a coarse approximation of the physiological complexity of plants [e.g. *Cramer et al.*, 1999, 2001; *Smith et al.*, 2008]. A full discussion on this topic is beyond the scope here, but it is worth mentioning the major weaknesses of the vegetation model used here. The first is the lack of simulation of plant hydraulics [e.g. *Katul et al.*, 2003; *Bohrer et al.*, 2005], which lead to simplified assumptions about xylem water dynamics and drought effects on plant functioning. The second is that the plant water uptake is not modeled in a fully three dimensional way [e.g. *Manoli et al.*, 2014] which could hinder elements of the spatial competition of plants for water. Third the effect of water variability on the nutritional status of the soil is also neglected since soil biogeochemistry is currently not resolved in *T&C*.

Moreover, the most important limitation is perhaps data availability. Even though meteorological and soil texture data existed, information concerning soil moisture, crust formation and presence, ET, runoff and spatial distribution of species composition was unavailable to further corroborate the presented results, as well as, hypotheses put forward by previous studies.

5. Conclusions

The ecohydrological behavior in terms of water and carbon fluxes of an ecosystem with an already established banded vegetation pattern has been explored. Numerical simulations with a

state-of-the-science model quantified the effects of precipitation, slope steepness, soil hydraulic properties and flow accumulation on the hydrological and plant physiological processes for idealized hillslopes and complex terrain where vegetation bands are present. The novelty of the study lies in the detailed and realistic representation of the ecohydrological processes at the appropriate scales. The work demonstrated the following points:

(a) Differently from several previous hypotheses, it was found that root-zone soil moisture within banded vegetation is on average lower when compared to their bare soil neighbors. This finding is explained by the enhanced ET resulting from the composite effect of bare soil evaporation and plant transpiration. However, immediately following a significant rainfall event, the opposite pattern emerges.

(b) Runoff generation, which primarily occurs on bare soils, provides an additional water subsidy to downstream vegetated areas given their higher infiltration capacity. The uphill part of each vegetation band benefits more from this process, suggesting the potential mechanism for uphill vegetation band migration. For significant runoff to occur in semi-arid areas, the existence of low permeability induced by soil sealing is essential. This is consistent with several but not all field observations in semi-arid and arid areas.

(c) Subsurface water flow, on average, leads to favorable soil water conditions at uphill and downhill edges of each vegetation band. The contribution of subsurface fluxes is almost comparable ($\sim$ 50% of the runoff contributions at the vegetation edges) to water contribution arising from overland flow at the study site.

(d) The small scale temporal dynamics of meteorological forcing, especially precipitation, plays a major role in determining the long term spatial distribution of soil moisture and cannot be neglected (Figure 8).

(e) The effect of complex topography mediates the various mechanisms leading to substantial differences in soil water availability and water fluxes between vegetated and bare soil areas. The differences in soil moisture for large flow accumulations (e.g. streams) is weakened (Figure 9), supporting the idea that plant competition for water, the driver of vegetation pattern formation, is mostly important on gently sloping hillsides of the catchments.

Acknowledgments

We thank Gopal G. Penny and Sally E. Thompson for their help with the data for the study. Meteorological for the Midlands airport data were obtained from (http://www.webmet.com), aerial photos were obtained by the National Agriculture Imagery Program (http://www.fsa.usda.gov/FSA/apfoapp?area=home&subject=prog&topic=nai), soil maps from USDA Soil Survey Geographic Database (http://www.nrcs.usda.gov/wps/portal/nrcs/detail/soils/survey/geo/?cid=nrcs142p2_053627) and the digital elevation model was obtained by the National Elavation Dataset of USGS (http://ned.usgs.gov/). A. Paschalis acknowledges the financial support of the Swiss National Sciences Foundation (grant No P2EZP2_152244) and the Stavros Niarchos Foundation, through the SNSF Early Postdoc Mobility Fellowship. G. Katul acknowledges support from the National Science Foundation (NSF-EAR-1344703, NSF-AGS-1102227, and NSF-CBET-103347), the United States Department of Agriculture (2011-67003-30222), the U.S. Department of Energy (DOE) through the office of Biological and Environmental Research (BER) Terrestrial Ecosystem Science (TES) Program (DE-SC0006967 and DE-SC0011461) and the Binational Agricultural Research and Development (BARD) Fund (IS-4374-11C). G. Manoli acknowledges support from the National Science Foundation (NSF-EAR-1344703).

Appendix A: *T&C* simplification details

In this appendix, further details on the two simplifications applied to the original formulation of *T&C* [*Fatichi et al.*, 2012a] are presented.

First, evapotranspiration is modeled according to *Shuttleworth and Wallace* [1985], where the estimation of latent heat flux depends on the meteorological conditions (relative humidity, incoming shortwave radiation, radiative and air temperature and wind speed), canopy properties (leaf area index, canopy height, radiative transfer in the canopy), ground and vegetation albedo values and atmospheric, stomatal, leaf boundary, soil and undercanopy resistances, and the radiative surface temperature is estimated according to *Iritz et al.* [1999]. In the present model, radiation transfer, surface albedo, ground heat flux, aerodynamics, undercanopy, leaf boundary and stomatal resistances are estimated identical to *T&C*. The only different component is for the soil resistance, which is estimated such that:

$$E_s(S_e) = (S_e)^{\zeta} E_s^{pot}, \tag{A1}$$

where $E_s(S_e)$ $[LT^{-1}]$ is the bare soil evaporation at effective soil moisture S_e $[-]$, E_s^{pot} $[LT^{-1}]$ the potential bare soil evaporation given a minimum reference soil resistance at saturation $r^s_{s_{ref}}$ $[TL^{-1}]$, and ζ $[-]$ an empirical parameter. This result leads to

$$r_s^s = (S_e^{-\zeta} - 1)(\Delta + \gamma)(r_a^a + r_a^s)/\gamma + (S_e^{-\zeta}) r^s_{s_{ref}}, \tag{A2}$$

when vegetation is present and

$$r_s^s = (S_e^{-\zeta} - 1)(\Delta + \gamma) r_a^a/\gamma + (S_e^{-\zeta}) r^s_{s_{ref}}, \tag{A3}$$

for the case of bare soil, where r_a^a $[TL^{-1}]$, r_a^s $[TL^{-1}]$ are the aerodynamic and undercanopy resistances, Δ $[ML^{-1}T^{-2}\Theta^{-1}]$ is the mean rate of change of saturated water vapor pressure with temperature, and γ $[ML^{-1}T^{-2}\Theta^{-1}]$ is the psychrometric constant.

The second modification is related to the subsurface flow. In the original formulation of *T&C*, the pressure gradient was approximated with the topographic gradient, and thus subsurface flow directions were fixed. In the present model, we approximate the depth averaged Richards equation with:

$$\frac{\partial \overline{\theta}}{\partial t} = \nabla \cdot q + S \approx \nabla \cdot \left(K(\overline{\theta}) \nabla H(\overline{\theta}) \right) + S \tag{A4}$$

where $\overline{\theta}$ $[L^3L^{-3}]$ is the depth averaged volumetric water content, q $[LT^{-1}]$ is the lateral soil water flux, H $[L]$ is the hydraulic head and S $[LT^{-1}]$ is the source/sink term equal to $S = I - ET - L$. The expression is exact only for the case of constant soil moisture in the root zone [*Kumar*, 2004]. Discretization of the equation in a regular grid was done similarly to *Mendicino et al.* [2006]; *Anagnostopoulos and Burlando* [2012] and was solved explicitly in time. The formulation of I is identical to *T&C* and leakage is modeled as free drainage, e.g., $L(\overline{\theta}) = K_{bot}(\overline{\theta})$, where $K_{bot}(\overline{\theta})$ is the unsaturated hydraulic conductivity of at the bottom of the root zone. This assumption corresponds to a unit gradient driving the flow at the bottom of the root-zone.

References

Abarbanel, H., R. Brown, J. Sidorowich, and L. Tsimring, The analysis of chaotic data in physical systems, *Reviews of Modern Physics*, *65*(4), 1331–1392, doi:10.1103/RevModPhys.65.1331, 1993.

Agassi, M., I. Shainberg, and J. Morin, Effect of electrolyte concentration and soil sodicity on infiltration rate and crust formation, *Soil Science Society of America Journal*, *45*(5), 848–851, doi:10.2136/sssaj1981.03615995004500050004x, 1981.

Anagnostopoulos, G. G., and P. Burlando, An Object-oriented computational framework for the simulation of variably saturated flow in soils, using a reduced complexity model, *Environmental Modelling & Software*, *38*, 191–202, doi:10.1016/j.envsoft.2012.06.002, 2012.

Assouline, S., Rainfall-induced soil surface sealing: A critical review of observations, conceptual models, and solutions, *Vadose Zone Journal*, *3*(2), 570–591, doi:10.2113/3.2.570, 2004.

Assouline, S., and Y. Mualem, Modeling the dynamics of seal formation and its effect on infiltration as related to soil and rainfall characteristics, *Water Resources Research*, *33*(7), 1527–1536, doi:10.1029/96WR02674, 1997.

Assouline, S., and Y. Mualem, Modeling the dynamics of soil seal formation: Analysis of the effect of soil and rainfall properties, *Water Resources Research*, *36*(8), 2341–2349, doi:10.1029/2000WR900069, 2000.

Assouline, S., and D. Or, Anisotropy factor of saturated and unsaturated soils, *Water Resources Research*, *42*(12), doi:10.1029/2006WR005001, 2006.

Barbier, N., P. Couteron, J. Lejoly, V. Deblauwe, and O. Lejeune, Self-organized vegetation patterning as a fingerprint of climate and human impact on semi-arid ecosystems, *Journal of Ecology*, *94*(3), 537–547, doi:10.1111/j.1365-2745.2006.01126.x, 2006.

710 Baudena, M., J. von Hardenberg, and A. Provenzale, Vegetation patterns and soilatmo-
711 sphere water fluxes in drylands, *Advances in Water Resources*, *53*, 131–138, doi:10.1016/
712 j.advwatres.2012.10.013, 2013.

713 Belnap, J., The potential roles of biological soil crusts in dryland hydrologic cycles, *Hydrologi-*
714 *cal Processes*, *20*(15), 3159–3178, doi:10.1002/hyp.6325, 2006.

715 Bhark, E. W., and E. E. Small, Association between Plant Canopies and the Spatial Patterns of
716 Infiltration in Shrubland and Grassland of the Chihuahuan Desert, New Mexico, *Ecosystems*,
717 *6*(2), 185–196, doi:10.1007/s10021-002-0210-9, 2003.

718 Bohrer, G., H. Mourad, T. a. Laursen, D. Drewry, R. Avissar, D. Poggi, R. Oren, and G. G.
719 Katul, Finite element tree crown hydrodynamics model (FETCH) using porous media flow
720 within branching elements: A new representation of tree hydrodynamics, *Water Resources*
721 *Research*, *41*(11), doi:10.1029/2005WR004181, 2005.

722 Bonan, G. B., S. Levis, L. Kergoat, and K. W. Oleson, Landscapes as patches of plant functional
723 types: An integrating concept for climate and ecosystem models, *Global Biogeochemical*
724 *Cycles*, *16*(2), 5–1–5–23, doi:10.1029/2000GB001360, 2002.

725 Borgogno, F., P. D'Odorico, F. Laio, and L. Ridolfi, Mathematical models of vegetation
726 pattern formation in ecohydrology, *Reviews of Geophysics*, *47*(RG1005), doi:10.1029/
727 2007RG000256.Ecohydrology, 2009.

728 Brisson, N., B. Itier, J. C. L'Hotel, and J. Y. Lorendeau, Parameterisation of the Shuttleworth-
729 Wallace model to estimate daily maximum transpiration for use in crop models, *Ecological*
730 *Modelling*, *107*(2-3), 159–169, doi:10.1016/S0304-3800(97)00215-9, 1998.

731 Bugmann, H., A review of forest gap models, *Climatic Change*, *51*(3-4), 259–305, 2001.

Caracciolo, D., L. V. Noto, E. Istanbulluoglu, S. Fatichi, and X. Zhou, Climate change and Ecotone boundaries: Insights from a cellular automata ecohydrology model in a Mediterranean catchment with topography controlled vegetation patterns, *Advances in Water Resources*, *73*, 159–175, doi:10.1016/j.advwatres.2014.08.001, 2014.

Cavanaugh, M., S. Kurc, and R. Scott, Evapotranspiration partitioning in semiarid shrubland ecosystems: a two-site evaluation of soil moisture control on transpiration, *Ecohydrology*, *4*, 671–681, doi:10.1002/eco, 2011.

Choudhury, B. J., and J. L. Monteith, A four-layer model for the heat budget of homogeneous land surfaces, *Quarterly Journal of the Royal Meteorological Society*, *114*(480), 373–398, doi:10.1002/qj.49711448006, 1988.

Couteron, P., Quantifying change in patterned semi-arid vegetation by Fourier analysis of digitized aerial photographs, *International Journal of Remote Sensing*, *23*(17), 3407–3425, doi:10.1080/01431160110107699, 2002.

Couteron, P., and O. Lejeune, Periodic spotted patterns in semi-arid vegetation explained by a propagation-inhibition model, *Journal of Ecology*, *89*(4), 616–628, doi:10.1046/j.0022-0477.2001.00588.x, 2001.

Couteron, P., A. Mahamane, P. Ouedraogo, and J. Seghieri, Differences between banded thickets (tiger bush) at two sites in West Africa, *Journal of Vegetation Science*, *11*(3), 321–328, 2000.

Cramer, W., D. W. Kicklighter, A. Bondeau, B. I. Moore, G. Churkina, B. Nemry, A. Ruimy, and A. Schloss, Comparing global models of terrestrial net primary productivity (NPP): overview and key results, *Global Change Biology*, *5*(S1), 1–15, 1999.

Cramer, W., et al., Global response of terrestrial ecosystem structure and function to CO_2 and climate change: results from six dynamic global vegetation models, *Global Change Biology*,

7(4), 357–373, doi:10.1046/j.1365-2486.2001.00383.x, 2001.

Daly, E., and A. Porporato, Impact of hydroclimatic fluctuations on the soil water balance, *Water Resources Research*, *42*(6), doi:10.1029/2005WR004606, 2006.

Deblauwe, V., N. Barbier, P. Couteron, O. Lejeune, and J. Bogaert, The global biogeography of semi-arid periodic vegetation patterns, *Global Ecology and Biogeography*, *17*(6), 715–723, doi:10.1111/j.1466-8238.2008.00413.x, 2008.

Deblauwe, V., P. Couteron, J. Bogaert, and N. Barbier, Determinants and dynamics of banded vegetation pattern migration in arid climates, *Ecological Monographs*, *82*(1), 3–21, 2012.

D'Odorico, P., F. Laio, and L. Ridolfi, Vegetation patterns induced by random climate fluctuations, *Geophysical Research Letters*, *33*(19), L19,404, doi:10.1029/2006GL027499, 2006a.

D'Odorico, P., F. Laio, and L. Ridolfi, Patterns as indicators of productivity enhancement by facilitation and competition in dryland vegetation, *Journal of Geophysical Research*, *111*(G3), G03,010, doi:10.1029/2006JG000176, 2006b.

D'Odorico, P., K. Caylor, G. S. Okin, and T. M. Scanlon, On soil moisturevegetation feedbacks and their possible effects on the dynamics of dryland ecosystems, *Journal of Geophysical Research*, *112*(G4), G04,010, doi:10.1029/2006JG000379, 2007.

Dunkerley, D., Banded vegetation: development under uniform rainfall from a simple cellular automaton model, *Plant Ecology*, *129*(2), 103–111, doi:10.1023/A:1009725732740, 1997.

Esteban, J., and V. Fairén, Self-organized formation of banded vegetation patterns in semi-arid regions: A model, *Ecological Complexity*, *3*(2), 109–118, doi:10.1016/j.ecocom.2005.10.001, 2006.

Fatichi, S., The modeling of hydrological cycle and its interaction with vegetation in the framework of climate change, Ph.D. thesis, University of Florence, University Braunschweig, 2010.

778 Fatichi, S., and V. Ivanov, Interannual variability of evapotranspiration and vegetation produc-
779 tivity, *Water Resources Research*, *50*(4), 3275–3294, doi:10.1002/2013WR015044, 2014.
780 Fatichi, S., and S. Leuzinger, Reconciling observations with modeling: The fate of water and
781 carbon allocation in a mature deciduous forest exposed to elevated CO_2, *Agricultural and*
782 *Forest Meteorology*, *174-175*, 144–157, doi:10.1016/j.agrformet.2013.02.005, 2013.
783 Fatichi, S., V. Y. Ivanov, and E. Caporali, A mechanistic ecohydrological model to investigate
784 complex interactions in cold and warm water-controlled environments: 1. Theoretical frame-
785 work and plot-scale analysis, *Journal of Advances in Modeling Earth Systems*, *4*(2), 1–31,
786 doi:10.1029/2011MS000086, 2012a.
787 Fatichi, S., V. Y. Ivanov, and E. Caporali, A mechanistic ecohydrological model to in-
788 vestigate complex interactions in cold and warm water-controlled environments: 2. Spa-
789 tiotemporal analyses, *Journal of Advances in Modeling Earth Systems*, *4*(2), 1–22, doi:
790 10.1029/2011MS000087, 2012b.
791 Fatichi, S., G. G. Katul, V. Y. Ivanov, C. Pappas, A. Paschalis, A. Consolo, J. Kim, and
792 P. Burlando, Abiotic and biotic controls of soil moisture spatio-temporal variability and
793 the occurrence of hysteresis, *Water Resources Research*, *51*(5), 3505–3524, doi:10.1002/
794 2014WR016102, 2015a.
795 Fatichi, S., C. Pappas, and V. Y. Ivanov, Modeling plantwater interactions: an ecohydrological
796 overview from the cell to the global scale, *Wiley Interdisciplinary Reviews: Water*, doi:10.
797 1002/wat2.1125, WATER-136.R1, 2015b.
798 Flores Cervantes, J. H., E. Istanbulluoglu, E. R. Vivoni, C. D. Holifield Collins, and R. L.
799 Bras, A geomorphic perspective on terrain-modulated organization of vegetation productivity:
800 analysis in two semiarid grassland ecosystems in Southwestern United States, *Ecohydrology*,

7(2), 242–257, doi:10.1002/eco.1333, 2014.

Foti, R., and J. a. Ramírez, A mechanistic description of the formation and evolution of vegetation patterns, *Hydrology and Earth System Sciences*, *17*(1), 63–84, doi:10.5194/hess-17-63-2013, 2013.

Francipane, A., V. Y. Ivanov, L. V. Noto, E. Istanbulluoglu, E. Arnone, and R. L. Bras, tRIBS-Erosion: A parsimonious physically-based model for studying catchment hydro-geomorphic response, *Catena*, *92*, 216–231, doi:10.1016/j.catena.2011.10.005, 2012.

Franz, T. E., K. K. Caylor, E. G. King, J. M. Nordbotten, M. a. Celia, and I. Rodríguez-Iturbe, An ecohydrological approach to predicting hillslope-scale vegetation patterns in dry-land ecosystems, *Water Resources Research*, *48*(1), W01,515, doi:10.1029/2011WR010524, 2012.

Friend, A., A. Stevens, R. Knox, and M. Cannell, A process-based, terrestrial biosphere model of ecosystem dynamics (Hybrid v3.0), *Ecological Modelling*, *95*(2-3), 249–287, doi:10.1016/S0304-3800(96)00034-8, 1997.

Garbrecht, J., and L. W. Martz, The assignment of drainage direction over flat surfaces in raster digital elevation models, *Journal of Hydrology*, *193*(1-4), 204–213, doi:10.1016/S0022-1694(96)03138-1, 1997.

Gerten, D., S. Schaphoff, U. Haberlandt, W. Lucht, and S. Sitch, Terrestrial vegetation and water balancehydrological evaluation of a dynamic global vegetation model, *Journal of Hydrology*, *286*(1-4), 249–270, doi:10.1016/j.jhydrol.2003.09.029, 2004.

Ghannam, K., T. Nakai, A. Paschalis, C. A. Oishi, A. Kotani, Y. Igarashi, T. Kumagai, and G. G. Katul, Persistence and memory time scales in root-zone soil moisture dynamics, *Water Resources Research*, *In Press*, doi:10.1002/2015WR017983, 2016.

824 Gilad, E., M. Shachak, and E. Meron, Dynamics and spatial organization of plant communities
825 in water-limited systems., *Theoretical population biology*, *72*(2), 214–230, doi:10.1016/j.tpb.
826 2007.05.002, 2007a.

827 Gilad, E., J. von Hardenberg, A. Provenzale, M. Shachak, and E. Meron, A mathematical model
828 of plants as ecosystem engineers., *Journal of theoretical biology*, *244*(4), 680–691, doi:10.
829 1016/j.jtbi.2006.08.006, 2007b.

830 Greene, R., Soil physical properties of three geomorphic zones in a semiarid mulga woodland,
831 *Australian Journal of Soil Research*, *30*(1), 55–69, doi:10.1071/SR9920055, 1992.

832 Guswa, A. J., M. Celia, and I. Rodríguez-Iturbe, Models of soil moisture dynamics in eco-
833 hydrology: A comparative study, *Water Resources Research*, *38*(9), 1166, doi:10.1029/
834 2001WR000826, 2002.

835 Gutiérrez-Jurado, H. a., E. R. Vivoni, C. Cikoski, J. B. J. Harrison, R. L. Bras, and E. Istanbul-
836 luoglu, On the observed ecohydrologic dynamics of a semiarid basin with aspect-delimited
837 ecosystems, *Water Resources Research*, *49*(12), 8263–8284, doi:10.1002/2013WR014364,
838 2013.

839 Guyot, G., C. Scoffoni, and L. Sack, Combined impacts of irradiance and dehydration on leaf
840 hydraulic conductance: insights into vulnerability and stomatal control, *Plant, Cell & Envi-*
841 *ronment*, *35*(5), 857–871, doi:10.1111/j.1365-3040.2011.02458.x, 2012.

842 Haghighi, E., E. Shahraeeni, P. Lehmann, and D. Or, Evaporation rates across a convective air
843 boundary layer are dominated by diffusion, *Water Resources Research*, *49*(3), 1602–1610,
844 doi:10.1002/wrcr.20166, 2013.

845 Haxeltine, A., and I. Prentice, BIOME3: An equilibrium terrestrial biosphere model based on
846 ecophysiological constraints, resource availability, and competition among plant functional

847 types, *Global Biogeochemical Cycles*, *10*(4), 693–709, doi:10.1029/96GB02344, 1996.

848 HilleRisLambers, R., M. Rietkerk, F. van den Bosch, H. H. T. Prins, and H. de Kroon, Vegetation
849 pattern formation in semi-arid grazing systems, *Ecology*, *82*(1), 50–61, 2001.

850 Hopp, L., S. Fatichi, and V. Y. Ivanov, Simulating water flow in variably saturated soils: A
851 comparison of a 3-D model with approximation based formulations, *Hydrology Research*,
852 doi:10.2166/nh.2015.126, 2015.

853 Hunter, N. M., M. S. Horritt, P. D. Bates, M. D. Wilson, and M. G. Werner, An adaptive time
854 step solution for raster-based storage cell modelling of floodplain inundation, *Advances in*
855 *Water Resources*, *28*(9), 975–991, doi:10.1016/j.advwatres.2005.03.007, 2005.

856 IPCC, Climate Change 2013 The physical science basis working group I Contribution to the fifth
857 assessment report of the Intergovernmental Panel on Climate Change, Cambridge University
858 Press, 2013.

859 Iritz, Z., A. Lindroth, M. Heikinheimo, A. Grelle, and E. Kellner, Test of a modified
860 Shuttleworth-Wallace estimate of boreal forest evaporation, *Agricultural and Forest Mete-*
861 *orology*, *98-99*, 605–619, doi:10.1016/S0168-1923(99)00127-6, 1999.

862 Katul, G., A. Porporato, R. Nathan, M. Siqueira, M. Soons, D. Poggi, H. Horn, and S. Levin,
863 Mechanistic analytical models for long-distance seed dispersal by wind, *The American natu-*
864 *ralist*, *166*(3), 368–381, 2005.

865 Katul, G. G., R. Leuning, and R. Oren, Relationship between plant hydraulic and biochemical
866 properties derived from a steady-state coupled water and carbon transport model, *Plant, Cell*
867 *and Environment*, *26*(3), 339–350, doi:10.1046/j.1365-3040.2003.00965.x, 2003.

868 Kefi, S., M. Rietkerk, C. L. Alados, Y. Pueyo, V. P. Papanastasis, A. Elaich, and P. C. de Ruiter,
869 Spatial vegetation patterns and imminent desertification in Mediterranean arid ecosystems.,

Nature, *449*(7159), 213–7, doi:10.1038/nature06111, 2007.

Kefi, S., M. Rietkerk, and G. G. Katul, Vegetation pattern shift as a result of rising atmospheric CO_2 in arid ecosystems., *Theoretical population biology*, *74*(4), 332–44, doi:10.1016/j.tpb.2008.09.004, 2008.

Kharin, V. V., F. W. Zwiers, X. Zhang, and M. Wehner, Changes in temperature and precipitation extremes in the CMIP5 ensemble, *Climatic Change*, *119*(2), 345–357, doi:10.1007/s10584-013-0705-8, 2013.

Klausmeier, C. A., Regular and Irregular Patterns in Semiarid Vegetation, *Science*, *284*(5421), 1826–1828, doi:10.1126/science.284.5421.1826, 1999.

Kletter, A. Y., J. von Hardenberg, E. Meron, and A. Provenzale, Patterned vegetation and rainfall intermittency., *Journal of theoretical biology*, *256*(4), 574–83, doi:10.1016/j.jtbi.2008.10.020, 2009.

Konings, A. G., S. C. Dekker, M. Rietkerk, and G. G. Katul, Drought sensitivity of patterned vegetation determined by rainfall-land surface feedbacks, *Journal of Geophysical Research*, *116*(G4), G04,008, doi:10.1029/2011JG001748, 2011.

Krinner, G., N. Viovy, N. de Noblet-Ducoudré, J. Ogée, J. Polcher, P. Friedlingstein, P. Ciais, S. Sitch, and I. C. Prentice, A dynamic global vegetation model for studies of the coupled atmosphere-biosphere system, *Global Biogeochemical Cycles*, *19*, GB1015, doi:10.1029/2003GB002199, 2005.

Kumar, P., Layer averaged Richard's equation with lateral flow, *Advances in Water Resources*, *27*(5), 521–531, doi:10.1016/j.advwatres.2004.02.007, 2004.

Kurc, S. a., and E. E. Small, Dynamics of evapotranspiration in semiarid grassland and shrubland ecosystems during the summer monsoon season, central New Mexico, *Water Resources*

Research, *40*(9), doi:10.1029/2004WR003068, 2004.

Laio, F., A. Porporato, L. Ridol, and I. Rodriguez-iturbe, Plants in water-controlled ecosystems : active role in hydrologic processes and response to water stress II . Probabilistic soil moisture dynamics, *Advances in Water Resources*, *24*(7), 707–723, 2001.

Lejeune, O., M. Tlidi, and R. Lefever, Vegetation spots and stripes: Dissipative structures in arid landscapes, *International Journal of Quantum Chemistry*, *98*(2), 261–271, doi:10.1002/qua.10878, 2004.

Leuning, R., A critical appraisal of a combined stomatalphotosynthesis model for C3 plants, *Plant, Cell & Environment*, *18*, 339–355, 1995.

Ludwig, J., B. Wilcox, D. Breshears, D. Tongway, and A. Imeson, Vegetation patches and runoff-erosion as interacting ecohydrological processes in semiarid landscapes, *Ecology*, *86*(2), 288–297, 2005.

Madsen, M. D., D. G. Chandler, and J. Belnap, Spatial gradients in ecohydrologic properties within a pinyon-juniper ecosystem, *Ecohydrolgy*, *1*, 349–360, doi:10.1002/eco, 2008.

Manoli, G., S. Bonetti, J.-C. Domec, M. Putti, G. Katul, and M. Marani, Tree root systems competing for soil moisture in a 3D soil-plant model, *Advances in Water Resources*, *66*, 32–42, doi:10.1016/j.advwatres.2014.01.006, 2014.

Mau, Y., L. Haim, A. Hagberg, and E. Meron, Competing resonances in spatially forced pattern-forming systems, *Physical Review E*, *88*(3), 032,917, doi:10.1103/PhysRevE.88.032917, 2013.

McDonald, A., R. Kinucan, and L. Loomis, Ecohydrological interactions within banded vegetation in the northeastern Chihuahuan Desert, USA, *Ecohydrology*, *2*(1), 66–71, doi:10.1002/eco.40, 2009.

McDowell, N., et al., Evaluating theories of drought induced vegetation mortality using a multimodelexperiment framework, *New Phytologist*, *200*(2), 304–321, doi:10.1111/nph.12465, 2013.

McDowell, N. G., D. J. Beerling, D. D. Breshears, R. a. Fisher, K. F. Raffa, and M. Stitt, The interdependence of mechanisms underlying climate-driven vegetation mortality., *Trends in ecology & evolution*, *26*(10), 523–32, doi:10.1016/j.tree.2011.06.003, 2011.

Mendicino, G., A. Senatore, G. Spezzano, and S. Straface, Three-dimensional unsaturated flow modeling using cellular automata, *Water Resources Research*, *42*(11), doi:10.1029/2005WR004472, 2006.

Moorcroft, P., G. Hurtt, and S. Pacala, A method for scaling vegetation dynamics: the ecosystem demography model (ED), *Ecological monographs*, *71*(4), 557–585, 2001.

Nathan, R., and H. Muller-Landau, Spatial patterns of seed dispersal, their determinants and consequences for recruitment., *Trends in ecology & evolution*, *15*(7), 278–285, 2000.

Noy-Meir, I., Desert ecosystems: environment and producers, *Annual review of ecology and systematics*, *4*(1973), 25–51, 1973.

Okin, G. S., and D. a. Gillette, Distribution of vegetation in wind-dominated landscapes: Implications for wind erosion modeling and landscape processes, *Journal of Geophysical Research: Atmospheres*, *106*(D9), 9673–9683, doi:10.1029/2001JD900052, 2001.

Or, D., P. Lehmann, E. Shahraeeni, and N. Shokri, Advances in Soil Evaporation Physics-A Review, *Vadose Zone Journal*, *12*(4), doi:10.2136/vzj2012.0163, 2013.

Pappas, C., Modeling terrestrial carbon and water dynamics, A critical appraisal and ways forward, Ph.D. thesis, ETH Zurich, Diss no. 22152, 2014.

938 Pappas, C., S. Fatichi, and P. Burlando, Modeling terrestrial carbon and water dynamics across
939 climatic gradients: does plant diversity matter?, *New Phytologist*, *In Press*, 2015a.
940 Pappas, C., S. Fatichi, S. Rimkus, P. Burlando, and M. O. Huber, The role of local scale het-
941 erogeneities in terrestrial ecosystem modeling, *Journal of Geophysical Research: Biogeo-*
942 *sciences*, *120*(2), doi:10.1002/2014JG002735, 2015b.
943 Paschalis, A., Modelling the space time structure of precipitation and its impact on basin re-
944 sponse, Ph.D. thesis, ETH Zurich, Diss no. 21112, 2013.
945 Paschalis, A., P. Molnar, S. Fatichi, and P. Burlando, On temporal stochastic modeling of pre-
946 cipitation, nesting models across scales, *Advances in Water Resources*, *63*, 152–166, doi:
947 10.1016/j.advwatres.2013.11.006, 2014.
948 Paschalis, A., S. Fatichi, G. G. Katul, and V. Y. Ivanov, Cross-scale impact of climate tem-
949 poral variability on ecosystem water and carbon fluxes, *Journal of Geophysical Research:*
950 *Biogeosciences*, *120*(9), 1716–1740, doi:10.1002/2015JG003002, 2015.
951 Penny, G. G., K. E. Daniels, and S. E. Thompson, Local properties of patterned vegetation :
952 quantifying endogenous and exogenous effects, *Philosophical transactions of the Royal So-*
953 *ciety of London. Series A, Mathematical, Physical & Engineering Sciences*, *371*(20120359),
954 doi:10.1098/rsta.2012.0359, 2013.
955 Rietkerk, M., and J. van de Koppel, Regular pattern formation in real ecosystems., *Trends in*
956 *ecology & evolution*, *23*(3), 169–75, doi:10.1016/j.tree.2007.10.013, 2008.
957 Rietkerk, M., M. Boerlijst, F. van Langevelde, R. HilleRisLambers, J. van de Koppel, L. Ku-
958 mar, H. H. T. Prins, and A. de Roos, Self-organization of vegetation in arid ecosystems, *The*
959 *American Naturalist*, *160*(4), 524–530, 2002.

960 Rietkerk, M., S. C. Dekker, P. C. de Ruiter, and J. van de Koppel, Self-organized patchiness
961 and catastrophic shifts in ecosystems., *Science (New York, N.Y.)*, *305*(5692), 1926–9, doi:
962 10.1126/science.1101867, 2004.
963 Rigon, R., G. Bertoldi, and T. M. Over, GEOtop: A Distributed Hydrological Model with
964 Coupled Water and Energy Budgets, *Journal of Hydrometeorology*, *7*(3), 371–388, doi:
965 10.1175/JHM497.1, 2006.
966 Saco, P. M., and M. Moreno-de las Heras, Ecogeomorphic coevolution of semiarid hillslopes:
967 Emergence of banded and striped vegetation patterns through interaction of biotic and abiotic
968 processes, *Water Resources Research*, *49*(1), 115–126, doi:10.1029/2012WR012001, 2013.
969 Saco, P. M., G. R. Willgoose, and G. R. Hancock, Eco-geomorphology of banded vegetation
970 patterns in arid and semi-arid regions, *Hydrology and Earth System Sciences*, *11*(6), 1717–
971 1730, doi:10.5194/hess-11-1717-2007, 2007.
972 Saxton, K. E., and W. J. Rawls, Soil Water Characteristic Estimates by Texture and Organic
973 Matter for Hydrologic Solutions, *Soil Science Society of America Journal*, *70*(5), 1569, doi:
974 10.2136/sssaj2005.0117, 2006.
975 Shen, C., and M. S. Phanikumar, A process-based, distributed hydrologic model based on a
976 large-scale method for surface-subsurface coupling, *Advances in Water Resources*, *33*(12),
977 1524–1541, doi:10.1016/j.advwatres.2010.09.002, 2010.
978 Shuttleworth, W., and R. Gurney, The theoretical relationship between foliage temperature and
979 canopy resistance in sparse crops, *Quarterly Journal of the Royal Meteorological Society*,
980 *116*, 497–519, 1990.
981 Shuttleworth, W., and J. Wallace, Evaporation from sparse crops - an energy combination
982 theory, *Quarterly Journal of the Royal Meteorological Society*, *111*(469), 839–855, doi:

983 10.1002/qj.49711146910, 1985.

984 Sillmann, J., V. V. Kharin, X. Zhang, F. W. Zwiers, and D. Bronaugh, Climate extremes indices
985 in the CMIP5 multimodel ensemble : Part 1 . Model evaluation in the present climate, *Journal*
986 *of Geophysical Research: Atmospheres*, *118*(4), 1–18, doi:10.1002/jgrd.50203, 2013.

987 Sitch, S., et al., Evaluation of ecosystem dynamics, plant geography and terrestrial carbon cy-
988 cling in the LPJ dynamic global vegetation model, *Global Change Biology*, *9*(2), 161–185,
989 doi:10.1046/j.1365-2486.2003.00569.x, 2003.

990 Sitch, S., et al., Evaluation of the terrestrial carbon cycle, future plant geography and climate-
991 carbon cycle feedbacks using five Dynamic Global Vegetation Models (DGVMs), *Global*
992 *Change Biology*, *14*(9), 2015–2039, doi:10.1111/j.1365-2486.2008.01626.x, 2008.

993 Smith, B., I. C. Prentice, and M. T. Sykes, Representation of vegetation dynamics in the mod-
994 elling of terrestrial ecosystems: comparing two contrasting approaches within European cli-
995 mate space, *Global Ecology and Biogeography*, *10*(6), 621–637, doi:10.1046/j.1466-822X.
996 2001.t01-1-00256.x, 2008.

997 Sperry, J. S., Hydraulic constraints on plant gas exchange, *Agricultural and Forest Meteorology*,
998 *104*(1), 13–23, doi:10.1016/S0168-1923(00)00144-1, 2000.

999 Thiery, J., J. D'Herbes, and C. Valentin, A model simulating the genesis of banded vegetation
1000 patterns in Niger, *Journal of Ecology*, *83*(3), 497–507, 1995.

1001 Thompson, S., G. Katul, and S. M. McMahon, Role of biomass spread in vegetation pat-
1002 tern formation within arid ecosystems, *Water Resources Research*, *44*(10), doi:10.1029/
1003 2008WR006916, 2008a.

1004 Thompson, S. E., and G. Katul, Secondary seed dispersal and its role in landscape organization,
1005 *Geophysical Research Letters*, *36*(2), doi:10.1029/2008GL036044, 2009.

Thompson, S. E., and G. G. Katul, Inferring ecosystem parameters from observation of vegetation patterns, *Geophysical Research Letters*, *38*(20), doi:10.1029/2011GL049182, 2011.

Thompson, S. E., G. G. Katul, and S. M. McMahon, Role of biomass spread in vegetation pattern formation within arid ecosystems, *Water Resources Research*, *44*(10), n/a–n/a, doi:10.1029/2008WR006916, 2008b.

Thompson, S. E., S. Assouline, L. Chen, A. Trahktenbrot, T. Svoray, and G. G. Katul, Secondary dispersal driven by overland flow in drylands: Review and mechanistic model development., *Movement ecology*, *2*(1), 7, doi:10.1186/2051-3933-2-7, 2014.

Ursino, N., The influence of soil properties on the formation of unstable vegetation patterns on hillsides of semiarid catchments, *Advances in Water Resources*, *28*(9), 956–963, doi:10.1016/j.advwatres.2005.02.009, 2005.

Ursino, N., Modeling banded vegetation patterns in semiarid regions: Interdependence between biomass growth rate and relevant hydrological processes, *Water Resources Research*, *43*(4), doi:10.1029/2006WR005292, 2007.

Valentin, C., J. D'Herbès, and J. Poesen, Soil and water components of banded vegetation patterns, *Catena*, *37*(1-2), 1–24, doi:10.1016/S0341-8162(99)00053-3, 1999.

van de Koppel, J., et al., Spatial heterogeneity and irreversible vegetation change in semiarid grazing systems., *The American naturalist*, *159*(2), 209–18, doi:10.1086/324791, 2002.

van Wijk, M. T., and I. Rodriguez-Iturbe, Tree-grass competition in space and time: Insights from a simple cellular automata model based on ecohydrological dynamics, *Water Resources Research*, *38*(9), 1179, doi:10.1029/2001WR000768, 2002.

Vico, G., et al., Climatic, ecophysiological, and phenological controls on plant ecohydrological strategies in seasonally dry ecosystems, *Ecohydrology*, *8*(4), 660–681, doi:10.1002/eco.1533,

2014.

Wagener, T., M. Sivapalan, P. Troch, and R. Woods, Catchment Classification and Hydrologic Similarity, *Geography Compass*, *1*(4), 901–931, doi:10.1111/j.1749-8198.2007.00039.x, 2007.

Yetemen, O., E. Instanbulluoglu, J. H. Flores Cervantes, E. R. Vivoni, and R. L. Bras, Ecohydrologic role of solar radiation on landscape evolution, *Water Resources Research*, *51*(2), 1127–1157, doi:10.1002/2014WR016169, 2015.

Zhou, M., H. Ishidaira, H. Hapuarachchi, J. Magome, A. Kiem, and K. Takeuchi, Estimating potential evapotranspiration using Shuttleworth-Wallace model and NOAA-AVHRR NDVI data to feed a distributed hydrological model over the Mekong River basin, *Journal of Hydrology*, *327*(1-2), 151–173, doi:10.1016/j.jhydrol.2005.11.013, 2006.

Table 1. Investigated variables of the 1-D hillslope numerical experiment

Parameters	Values
Slope [%]	0.5
	1
	2.5
	5
Soil Properties (%sand-%clay-%silt-%organic; K_{sat} [mm h^{-1}])	*bare patch, vegetated patch*
	(42.8-8.7-47.5-1; 27), (42.8-8.7-44.5-4; 51)
	(6.8-31.5-60.7-1; 3), (6.8-31.5-57.7-4; 12)

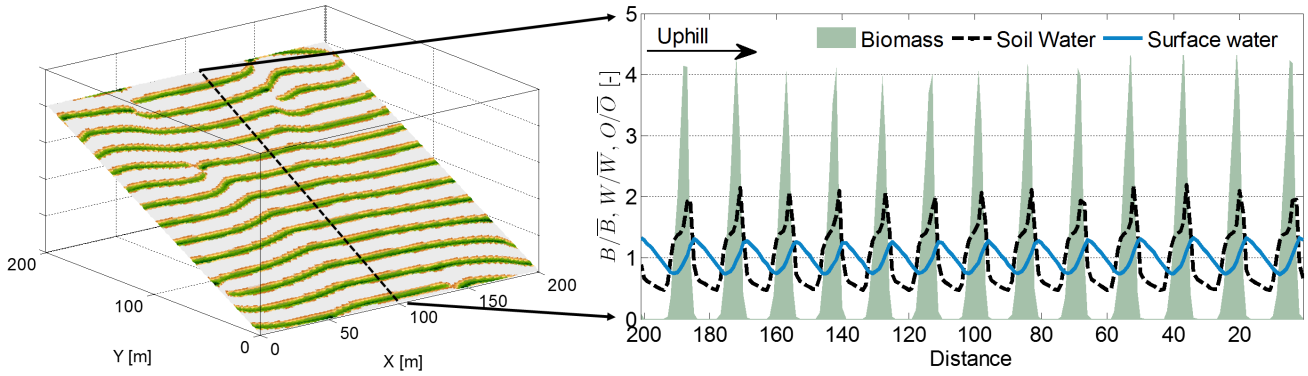

Figure 1. A vegetation pattern realization computed with the model presented in *Rietkerk et al.* [2002]. The left panel shows the spatial distribution of the simulated vegetation bands (green) and the right panel shows a cross-section of the hillpslope where the normalized biomass ($B/\overline{B}$ $[-]$), soil water ($W/\overline{W}$ $[-]$) and surface water ($O/\overline{O}$ $[-]$) are shown.

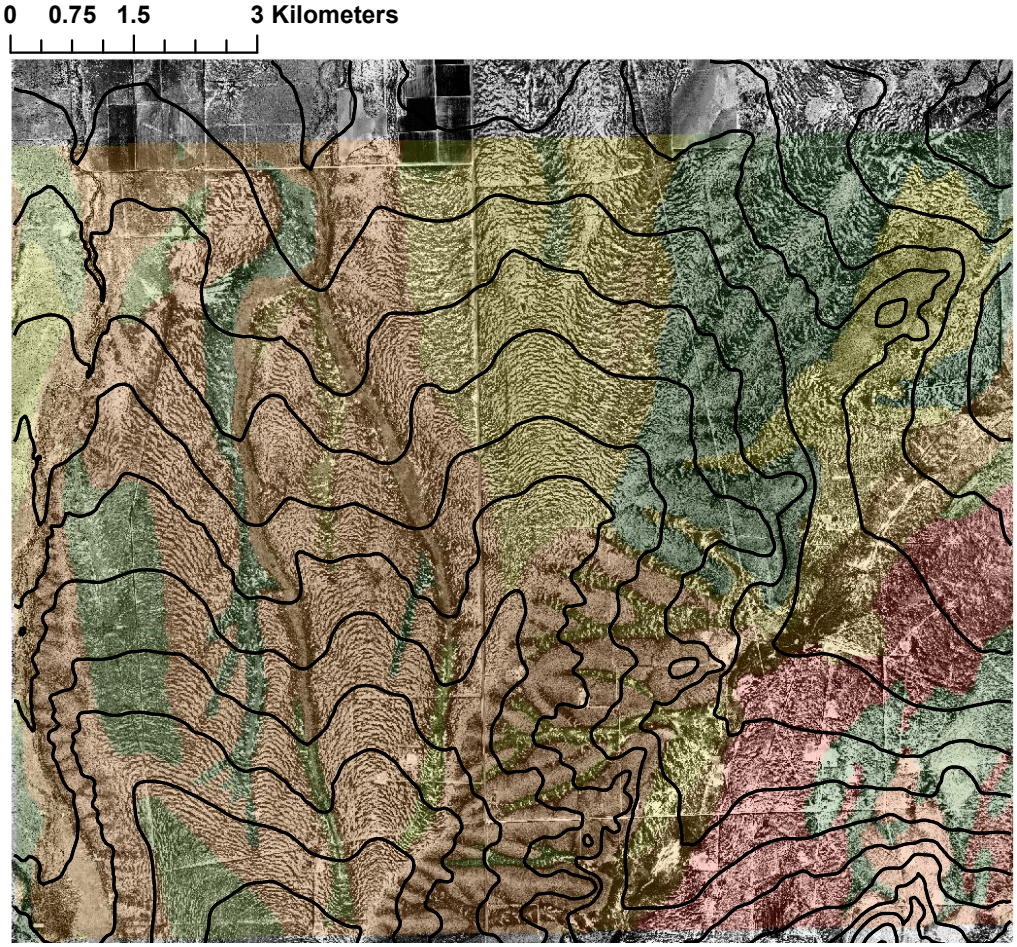

Figure 2. Aerial photograph of the study domain. Dark colors indicate vegetation. Different transparent colors show the various soil types in the area, and the lines correspond to 5 m elevation contours.

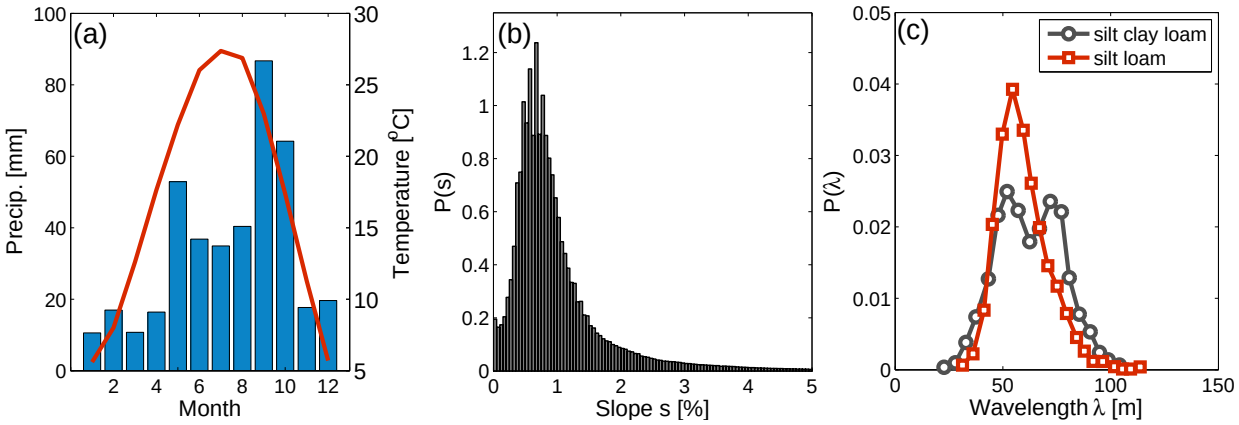

Figure 3. (a) Monthly variation of precipitation and temperature measured at the Midlands airport weather station. (b) Probability density function of the local DEM slopes estimated as the steepest neighbor descent (D8 algorithm [*Garbrecht and Martz*, 1997]). (c) Probability density of the vegetation band periodicity wavenumber estimated with a local 2D Fourier transform in *Penny et al.* [2013]. The 2 lines correspond to the 2 dominant soil types in the catchment.

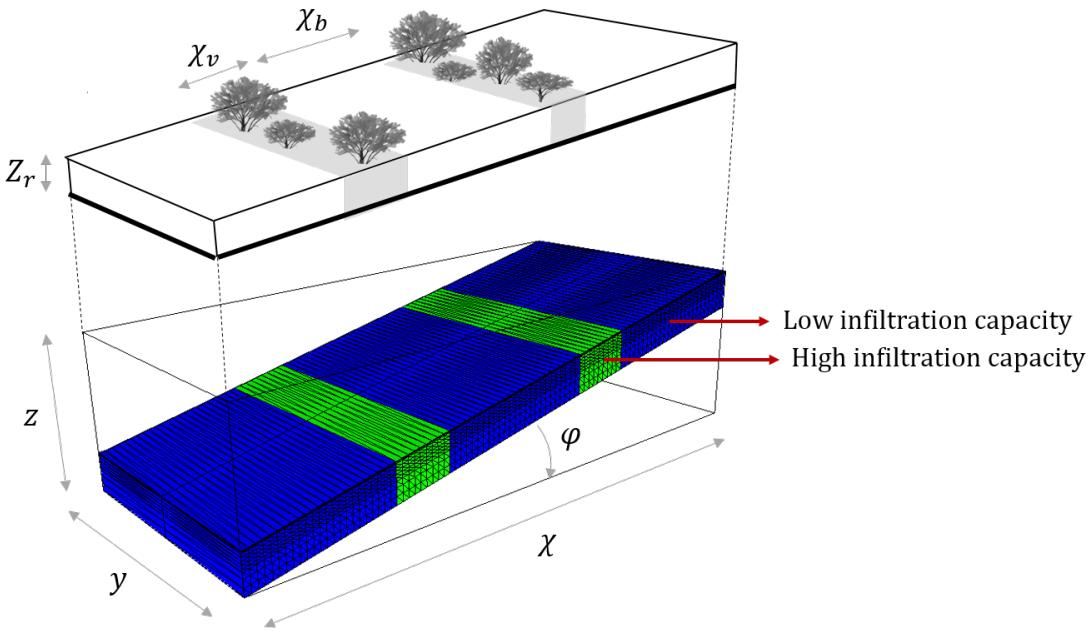

Figure 4. Schematic representation of the idealized slope for the numerical experiments.

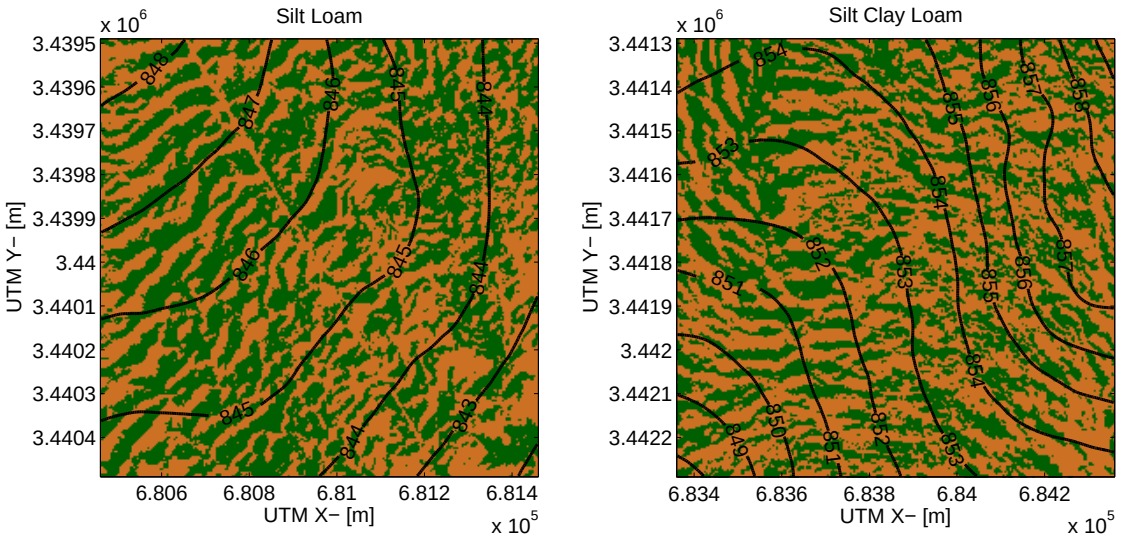

Figure 5. Aerial photography for the two simulation domains. Green represents existing vegetation, and yellow bare soil. Contour lines show the elevation in [m].

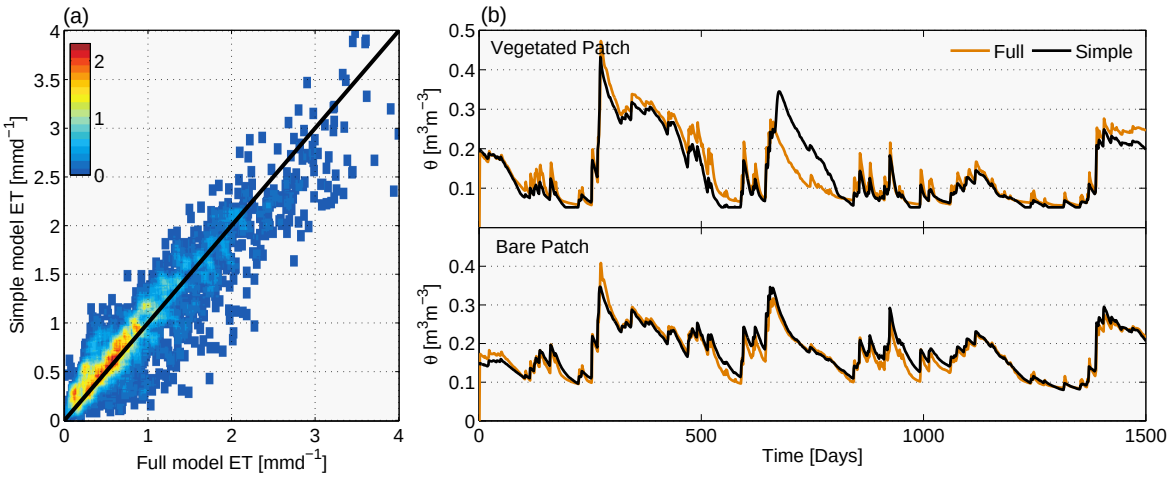

Figure 6. Comparison between the full version of the *T&C* model and its simplified version used for this study. (a) A scatter plot of the daily ET averaged across the simulation hillslope between the two models. The colors indicate the probability density. (b) A comparison of soil moisture for a vegetated patch (upper panel) and a bare soil patch (lower panel).

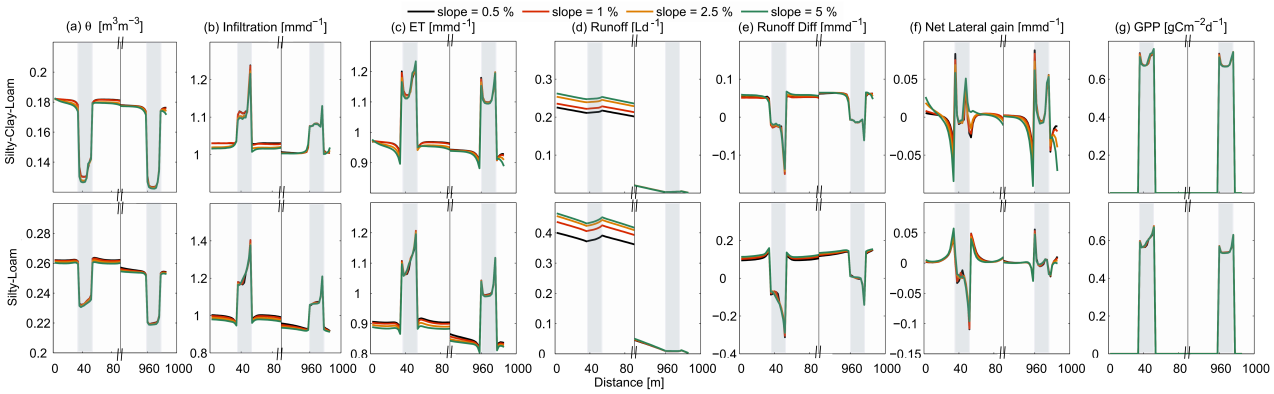

Figure 7. Profiles of the average (a) soil water content, (b) Infiltration, (c) ET, (d) Overland flow, (e) Difference between outgoing and incoming overland flow per computational cell, (f) net water gain from subsurface water routing, and (g) GPP on the idealized hillslope. Different colors represent the magnitude of the slope. The left part of each panel shows the vegetation band on the foot of the hillslope where overland flow accumulation is maximum, and the right part the vegetation band on the top of the slope, where overland flow accumulation is minimum. The location of the vegetation pattern is indicated with a shaded grey area.

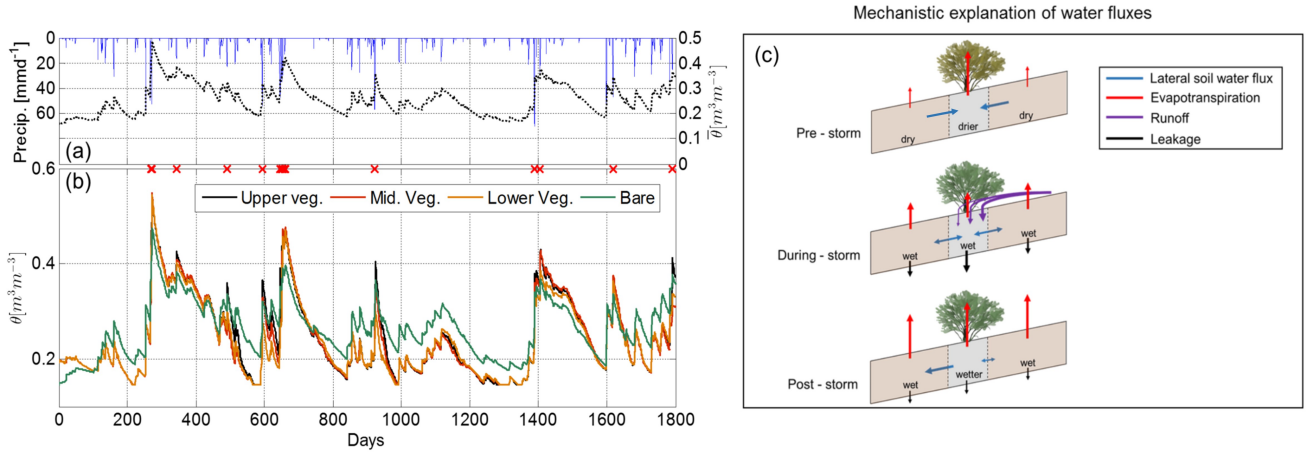

Figure 8. Temporal evolution of soil water content for the idealized slope with 1% inclination and soil type 1 for 5 years of simulation. (a) The observed precipitation series, and the simulated average soil water content on the hillslope. The temporal evolution of soil water content for the upper, middle and lower part of a vegetation band, and the adjacent bare soil is shown in panel (b). Red crosses show the timing of occurrence of the strongest 25% runoff events in the bare soil. In panel (c) a schematic representation of the water fluxes for a vegetation band is shown. Arrow directions represent the direction of each of the water fluxes according to the legend, and their thickness represents their relative magnitude.

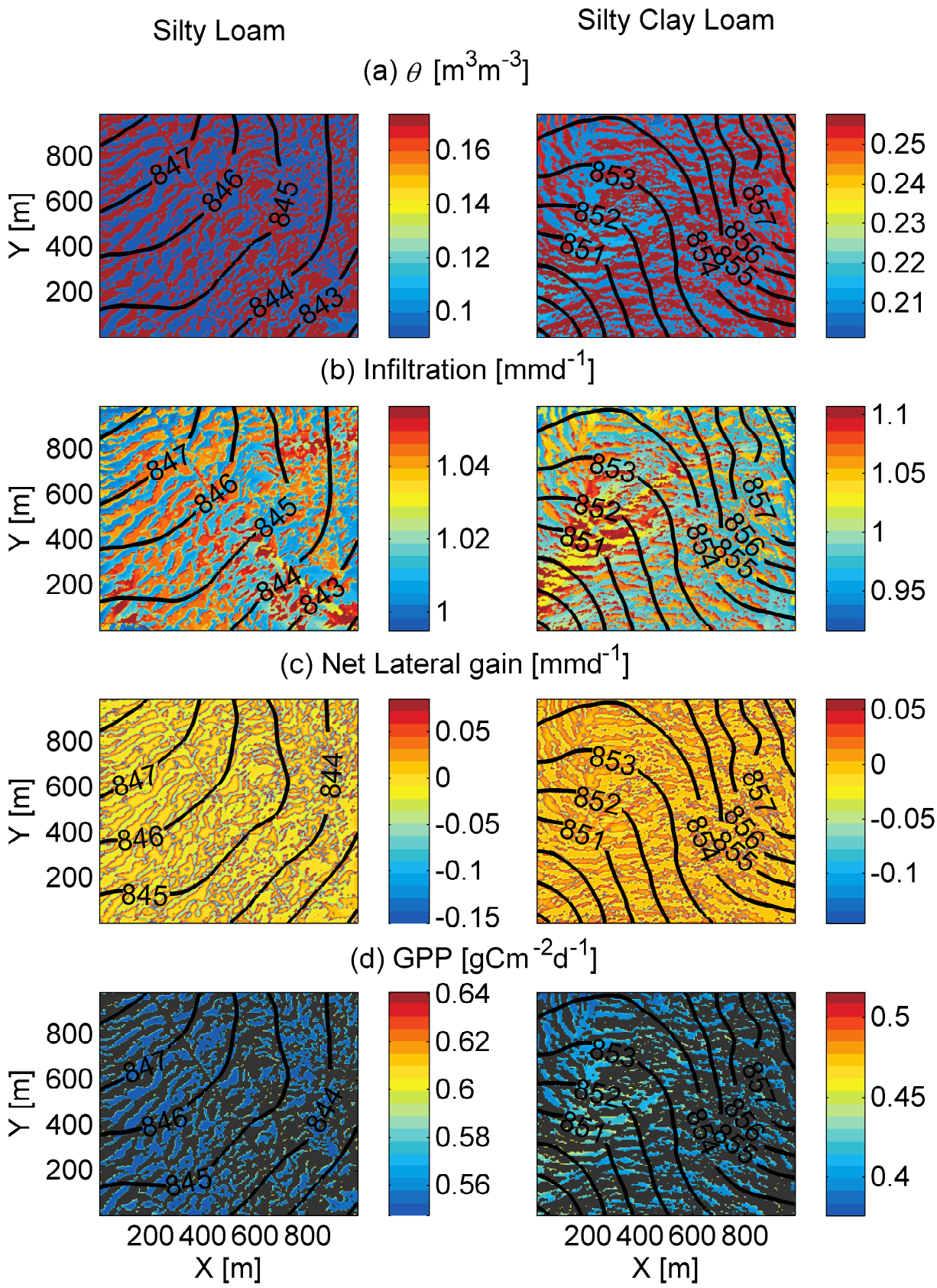

Figure 9. Spatial distribution of (a) soil water content, (b) infiltration, (c) net subsurface water gain, and (d) GPP for the two simulated areas. Gray color in (d) represents not vegetated areas